NASA TECHNICAL NOTE

NASA TN D-5583

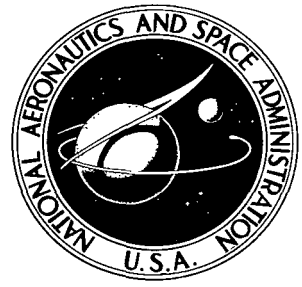

MEASUREMENTS OF DIELECTRIC CONSTANTS AND LOSS TANGENTS AT E-BAND USING A FABRY-PEROT INTERFEROMETER

by Constantine A. Balanis

Langley Research Center
Langley Station, Hampton, Va.

NATIONAL AERONAUTICS AND SPACE ADMINISTRATION • WASHINGTON, D. C. • DECEMBER 1969

1. Report No. NASA TN D-5583	2. Government Accession No.	3. Recipient's Catalog No.
4. Title and Subtitle MEASUREMENTS OF DIELECTRIC CONSTANTS AND LOSS TANGENTS AT E-BAND USING A FABRY-PEROT INTERFEROMETER		5. Report Date December 1969 6. Performing Organization Code
7. Author(s) Constantine A. Balanis		8. Performing Organization Report No. L-6881
9. Performing Organization Name and Address NASA Langley Research Center Hampton, Va. 23365		10. Work Unit No. 125-21-04-01-23 11. Contract or Grant No. 13. Type of Report and Period Covered Technical Note
12. Sponsoring Agency Name and Address National Aeronautics and Space Administration Washington, D.C. 20546		14. Sponsoring Agency Code

15. Supplementary Notes Part of the material contained in this report was also submitted as a thesis entitled "Investigation of a Proposed Technique for Measurements of Dielectric Constants and Losses at V-Band Using the Fabry-Perot Principle" in partial fulfillment of the requirements for the Degree Master of Electrical Engineering, University of Virginia, Charlottesville, Virginia, August 1966.

16. Abstract

Dielectric constant and loss tangent measurements for polytetrafluoroethylene (teflon), polystyrene, and polymethyl methacrylate (lucite, plexiglas) were made at E-band (≈60 to 90 GHz) using a Fabry-Perot interferometer. These measurements provided experimental data not previously available at these frequencies. In addition, they provided further verification of the use of the Fabry-Perot interferometer as an effective instrument for measuring dielectric constants and loss tangents in the millimeter wavelength region. Samples of various thicknesses and surface finishes were used to determine the effect of these variables on the measurements. To determine the variation of dielectric constants with temperature, measurements were made over a limited temperature range and a reduction in value was observed at higher temperatures.

17. Key Words Suggested by Author(s) Dielectric constants Loss tangents Fabry-Perot interferometer	18. Distribution Statement Unclassified – Unlimited		
19. Security Classif. (of this report) Unclassified	20. Security Classif. (of this page) Unclassified	21. No. of Pages 51	22. Price* $3.00

*For sale by the Clearinghouse for Federal Scientific and Technical Information
Springfield, Virginia 22151

MEASUREMENTS OF DIELECTRIC CONSTANTS AND LOSS TANGENTS AT E-BAND USING A FABRY-PEROT INTERFEROMETER*

By Constantine A. Balanis
Langley Research Center

SUMMARY

Dielectric constant and loss tangent measurements for polytetrafluoroethylene (teflon), polystyrene, and polymethyl methacrylate (lucite, plexiglas) were made at E-band (≈60 to 90 GHz) using a Fabry-Perot interferometer. These measurements provided experimental data not previously available at these frequencies. In addition, they provided further verification of the use of the Fabry-Perot interferometer as an effective instrument for measuring dielectric constants and loss tangents in the millimeter wavelength region.

Samples of various thicknesses and surface finishes were used to determine the effect of these variables on the measurements. To determine the variation of dielectric constants with temperature, measurements were made over a limited temperature range and a reduction in value was observed at higher temperatures.

INTRODUCTION

A dielectric material can react to an electric field because it contains charge carriers that can be displaced. This polarization phenomenon is a function of frequency, as shown in figure 1. (See ref. 1.) Since the dielectric constant is proportional to the polarization of a material, it will also be a function of frequency. However, since the calculation of dielectric properties of material is very difficult, they must be measured experimentally. (See ref. 2.) Dielectric constant and loss tangent values have been measured and tabulated extensively up to the centimeter wavelength region (ref. 3), but very few measurements have been made in the millimeter and submillimeter wavelength regions. (See refs. 4 to 8.)

---

*Part of the material contained in this report was also submitted as a thesis entitled "Investigation of a Proposed Technique for Measurements of Dielectric Constants and Losses at V-Band Using the Fabry-Perot Principle" in partial fulfillment of the requirements for the Degree Master of Electrical Engineering, University of Virginia, Charlottesville, Virginia, August 1966.

In the millimeter and submillimeter wavelength regions, conventional microwave cavity resonators become increasingly difficult to construct while maintaining relative high cavity quality factors (Q), as their dimensions must be comparable with the operating wavelength. To avoid these difficulties, optical resonators such as the Fabry-Perot interferometer (see fig. 2) can be used with dimensions many times larger than the operating wavelength. The Fabry-Perot interferometer has been used extensively as a resonator at optical frequencies and has been investigated as a microwave cavity for use in the millimeter region. (See refs. 9 to 12.) Fabry-Perot techniques have been applied for measurements of dielectric properties at 47 GHz (ref. 5), 143 GHz, and 343 GHz (ref. 8). The author also has utilized the Fabry-Perot system for the investigation of dielectric properties of materials at 60 GHz, by using phase-lock techniques for cavity quality factor measurements. (See ref. 6.)

For the present investigation, the Fabry-Perot interferometer was used for measurements of dielectric constants and loss tangents for teflon, polystyrene, and lucite in the 60 to 90 GHz region. Two methods were used for the measurements of dielectric constants. One method can be used for making measurements on samples of any thickness at any frequency whereas the other can only be used when the effective slab thickness is an integral number of a half-wavelength. Loss tangent measurements were made only on samples whose thickness was an integral number of a half-wavelength. To determine the effects of surface irregularities on the measurements, samples of different thickness and surface finish were used and the results were compared.

SYMBOLS

A	surface area of reflector plate
A_i, B_i	amplitudes of electric and magnetic fields in different regions
E	electric-field intensity
E^*	conjugate of electric-field intensity
E_i	electric-field intensity in different regions
H	magnetic-field intensity
H^*	conjugate of magnetic-field intensity

H_i magnetic-field intensity in different regions

H_{tan} magnetic-field intensity tangential to plate surface

H^*_{tan} conjugate of tangential magnetic field

P polarization

P_d diffraction losses

P_s dissipated power in cavity

P_{atomic} atomic polarization

$P_{dipolar}$ dipolar polarization

$P_{electronic}$ electronic polarization

Q cavity quality factor

Q_o quality factor of cavity without dielectric sheet

Q_t quality factor of cavity when dielectric sheet is an integral number of a half-wavelength

$Q_{t,max}$ maximum quality factor of cavity when dielectric sheet is an integral number of a half-wavelength

$R(s)$ real part of surface impedance of plates

V volume of cavity

W_s stored energy in cavity

Z_i impedances in different regions

Z_L load impedance

a,b	distances between centers of coupling holes in y- and z-directions
d	plate separation
dS	differential plate surface area
dV	differential cavity volume
f_o	resonance frequency, cycles per second
i	an integer subscript
$j = \sqrt{-1}$	
k	index of refraction
n	a constant
r	radius of hole in reflector plate
s_1	slab thickness
s_2, s_3	relative distances between dielectric sheet and plate 2
t	time
t_o	transmission coefficient
t_{12}	transmission coefficient from region 2 to 1
t_{21}	transmission coefficient from region 1 to 2
t_{32}	transmission coefficient from region 2 to 3
x,y,z	rectangular coordinates
x_i	position along x-axis

α	attenuation constant
β	phase constant in free space
β_1	phase constant of dielectric sheet
γ	reflection and diffraction losses
ϵ	dielectric constant
ϵ_i	permittivity constant
ϵ'	real part of dielectric constant
ϵ''	imaginary part of dielectric constant
λ	wavelength in free space
λ_1	wavelength in dielectric sheet
μ_i	permeability constant
ρ_i	reflection coefficient
ω	angular frequency
tan δ	loss tangent
Δ	differential shift necessary to restore resonance
Δf	half-power bandwidth of cavity response, cycles per second
Δ_{max}	maximum differential shift necessary to restore resonance
Δ_{min}	minimum differential shift necessary to restore resonance
$\sqrt{}$	SAE surface symbol indicating average root-mean-square height of surface irregularities in microinches

SYSTEM DESCRIPTION

A photograph and a block diagram of the system used for the measurements are shown in figures 3 and 4, respectively. The basic frame of the interferometer is 36 inches (914.4 mm) long. Two upright frames are used to support the reflector plates; each plate has various tilt adjustment and a mechanism for translation relative to the other plate. Tilt adjustments are needed for parallel alinement of the reflector plates necessary to reduce diffraction losses. The middle upright frame is used to support the dielectric slabs, and it also has various tilt adjustments. The aperture of the middle frame is 10 by 10 inches (254 by 254 mm) so that dielectric slabs larger than the size of the reflector plates can be used.

The horn antennas have an aperture of $2\frac{1}{8}$ by $2\frac{1}{8}$ inches (53.98 by 53.98 mm). The dielectric lenses were used to convert spherical waves to plane waves. To couple energy in and out of the cavity, coupling holes on very thin reflector plates were employed. (See ref. 12.) The perforated membranes, 0.001 inch (0.0254 mm) thick, were used for the reflectors. They were made of nickel and were coated with a thin film of gold to increase the conductivity of the surface and to prevent corrosion. A photoetching process was used for the construction of the membranes which are circular in shape with a diameter of about 5 inches (127 mm). A photograph of a membrane used in the tests is shown in figure 5. The hole pattern of the perforated membranes is shown better in figure 6 with pertinent dimensions of $a = b = 0.1$ inch (2.54 mm) and $r = 0.02$ inch (0.508 mm).

INTERFEROMETER RESONANCE THEORY

The resonance of a Fabry-Perot cavity occurs when the plate separation is an integral number of a half-wavelength. (See appendix B, eq. (63).) Once resonance is obtained, the insertion of a dielectric slab between the plates will disturb the resonance condition, and a shift in plate position is needed to restore it.

The equation describing interferometer resonance condition can be derived by applying boundary conditions at points of discontinuity (refs. 5 and 13). However, the same equations can be derived more conveniently by using transmission line theory as shown in appendix A. It should be pointed out that by using transmission line theory, all details describing field variations at points of discontinuity are lost. Reference to figure 7(a) shows that the resulting equation for resonance

$$k\left(\cot \beta s_2 + \cot \beta x_1\right)\cot \beta_1 s_1 + \cot \beta x_1 \cot \beta s_2 - k^2 = 0 \tag{1}$$

is a function of relative spacing and index of refraction.

By using the notation of figure 7(b), it is shown by equation (35) that the shift of plate 2 necessary to restore resonance Δ is a function of dielectric slab position s_3. The maximum and minimum values of Δ (appendix A, eqs. (38) and (39)) are given by

$$\tan \frac{1}{2}\beta(s_1 + \Delta) = \frac{1}{k}\left[\tan\left(\frac{1}{2}\beta_1 s_1\right)\right] \tag{2}$$

$$\tan \frac{1}{2}\beta(s_1 + \Delta) = k\left[\tan\left(\frac{1}{2}\beta_1 s_1\right)\right] \tag{3}$$

The sign of $\tan \frac{\beta_1 s_1}{2}$ determines which of equations (2) or (3) represents Δ_{max} or Δ_{min}. Since $k > 1$, it is evident that when the integral part of $2s_1/\lambda_1$ is zero or an even integer, equation (2) gives Δ_{min} and equation (3) gives Δ_{max}; when the integral part of $2s_1/\lambda_1$ is an odd integer, equation (2) gives Δ_{max} and equation (3) gives Δ_{min}.

When the dielectric sheet thickness is a multiple of a half-wavelength, the equation defining resonance (see appendix A, eq. (42)) reduces to

$$\Delta = s_1(k - 1) \tag{4}$$

It should be pointed out that these derivations will not apply for highly conductive slabs because it was assumed that $\mu_o \approx \mu_1$.

The equation for determining the loss tangent is

$$\frac{1}{Q_{t,max}} = \frac{1}{Q_o} + \left(\frac{s_1}{d}\right)\tan \delta \tag{5}$$

where $Q_{t,max}$ is the maximum value of the quality factor when the sheet thickness is an integral number of a half-wavelength. Equation (5) is derived in appendix A by assuming that slabs whose thicknesses are a multiple of a half-wavelength are used and that the diffraction losses with and without the slab between the reflector plates are the same.

EXPERIMENTAL TECHNIQUE AND ANALYTIC PROCEDURE

Measurement of Q

Conventional methods employed for the measurements of Q at lower microwave frequencies (ref. 2) cannot be used in the millimeter region since accurate wave meters are not presently available. A different system for obtaining the Fabry-Perot cavity Q is presented here. The E-band klystron of figure 4 is linearly varied through a small frequency range, and the response of the Fabry-Perot resonant cavity is displayed on the oscilloscope. Such a response curve is shown in figure 8(a). A portion of the output of

the E-band klystron is mixed with a harmonic of the phase-locked X-band source which is varied until a zero beat is detected from the harmonic mixer. The zero beat is displayed simultaneously on a dual-beam oscilloscope with the response of the cavity, and it is used as a variable-frequency marker which is tuned to the center frequency and then to each of the half-power bandwidth points of the response curve. The zero beat used as a frequency marker is shown in figure 8(b). The frequency for each position of the marker is determined for each case by measuring the frequency of the 15 to 15.125 MHz radio frequency (rf) reference crystal oscillator with a 50 MHz counter; thus, accurate determination of the center frequency and the half-power bandwidth of the cavity response was possible. The Q of the cavity is then determined by

$$Q = \frac{f_o}{\Delta f} \tag{6}$$

where

f_o center frequency of cavity response

Δf half-power bandwidth of cavity response

Dielectric Constants Measurements

Two methods were used for the measurement of dielectric constants, and the analytical procedure for each is discussed. The second method would be the easiest to use if the operating frequency can be varied to obtain an integral number of half-wavelengths in the slab to be measured. When it is necessary to measure dielectric constants at a specified frequency so that it is not possible to adjust frequency to make the available slabs an integral number of half-wavelengths, the first method must be used.

First method.- The equations for determining the dielectric constant by using this method (see appendix A) are

$$\tan \frac{1}{2}\beta(s_1 + \Delta) = \frac{1}{k}\tan\left(\frac{1}{2}\beta_1 s_1\right) \tag{7}$$

$$\tan \frac{1}{2}\beta(s_1 + \Delta) = k\tan\left(\frac{1}{2}\beta_1 s_1\right) \tag{8}$$

There are many values of k which will satisfy equations (7) and (8), but there is only one value which will be the same for the different thickness slabs. If the approximate range of k is known beforehand, it is not necessary to find all the possible k values which satisfy equations (7) and (8) for each slab but instead one could concentrate only on the known range. However, if no previous knowledge of the range of k is known,

many k values for each slab must be found and compared. Before using equations (7) and (8) for determining the dielectric constant, a plot of the position shift of plate 2 necessary to restore resonance Δ against dielectric position s_3 must be drawn to determine Δ_{max} and Δ_{min}. An experimental plot is shown in figure 9.

Once Δ_{max} and Δ_{min} are determined, an iterative procedure ideally suited for use with a computer (ref. 6) is applied for determining k by using equations (7) and (8). It must be remembered that whether Δ_{max} or Δ_{min} is used with equations (7) or (8) depends upon the integral part of $2s_1/\lambda_1$. (See appendix A.) To avoid any possible errors, equations (7) and (8) and $2s_1/\lambda_1$ were evaluated for each value of Δ_{max} and Δ_{min}. The correct value of k was determined by checking each value of Δ_{max} or Δ_{min} against its corresponding value of $2s_1/\lambda_1$.

Second method.- Slabs whose thicknesses are a multiple of a half-wavelength must be used. To make sure that the effective slab thickness is a multiple of a half-wavelength, a change in the position of the slab during resonance conditions should not disturb resonance. This fact can be understood by remembering that the impedance before and after the slab is the same. So, the Δ required to restore resonance by use of this method is the same for any position relative to the reflectors of the dielectric slab. Equation (4) which gives the index of refraction can be written

$$k = 1 + \frac{\Delta}{s_1} \tag{9a}$$

where

$$s_1 = \frac{n\lambda}{2} \qquad (n = 1, 2, 3, \ldots) \tag{9b}$$

As the slab thickness varies, Δ will also vary. The Δ used with equation (9a) to determine k must be carefully selected. For each slab there are many values of Δ which restore resonance, and they are spaced one-half wavelength apart. To select the correct Δ, various thickness slabs are used, and for each slab, successive Δ values and their corresponding k values are determined. By comparing the k values of the different thickness slabs of the same material, it is evident that only one value of k is the same for each thickness. If the slab thickness is equal to a half-wavelength ($n = 1$), the first Δ will give the correct answer.

Loss Tangent Measurements

Before loss tangent measurements were made, experimental curves of Q against plate separation were plotted and they are shown in figure 10. These curves closely resemble the predicted shapes. (See appendix B.) No data could be taken for plate separations less than about 5 inches (127 mm) because of the presence of the middle frame.

There exists a linear relation between Q and plate position with air for separations up to about 7 inches (177.8 mm). This linear relation is an indication of the small effect of the diffraction losses in that region. As the plate separation is increased further, the diffraction losses become noticeable and the experimental curve is flattened. The curves with the different dielectrics between the plates begin to flatten at smaller plate separations. This flattening indicates that diffraction losses become noticeable at shorter plate separations, possibly because of the surface imperfections of the dielectrics and diffraction from the edges of the dielectric sheet and frames. The cavity responses with each material between its plates are shown in figure 11.

Diffraction losses cannot be calculated, but at close plate separations they should be small. To simplify the calculations of the loss tangent, it was assumed that diffraction losses with and without the dielectric are the same and that slabs whose thickness are multiples of half-wavelengths were used. The equation used for determining the loss tangent is

$$\frac{1}{Q_{t,max}} = \frac{1}{Q_o} + \left(\frac{s_1}{d}\right)\tan \delta \tag{10}$$

To determine $Q_{t,max}$, a plot of the variation of Q with plate position must be drawn. An experimental curve is shown in figure 12. Once $Q_{t,max}$ is determined, the Q_o without the slab must be measured with the same position and spacing between the plates. These two values along with the slab thickness and plate separation can be used with equation (10) to determine $\tan \delta$.

Accuracy

The quantities used in the calculation of the index of refraction (eqs. (7), (8), and (9)) were slab thickness s_1, shift of plate position to restore resonance Δ, and phase constant (β-function of frequency). It was possible to measure s_1 and Δ within 0.001 inch (0.0254 mm). For such accuracies in the measurements, the values of the dielectric constants were within 1 percent or better. Frequency stabilities of only one part in 10^4 were necessary for this accuracy.

The accuracy of the loss tangent is governed by the accuracy of the Q values and dimension measurements. (See eq. (10).) In general, it was possible to measure the half-power bandwidth points repeatedly to about ±3 percent and dimension measurements to within 0.001 inch (0.0254 mm). The values of loss tangents obtained with such accuracies were within ±15 percent.

RESULTS AND DISCUSSION

The dielectric constants obtained by using the first and second methods are shown in tables I and II, respectively, and the loss tangents in table III. The values of the dielectric constants and loss tangents of the same material with different surface finishes obtained are within the stated accuracies. Thus, the variations of the dielectric constants and loss tangents of slabs with different surface finishes used in this investigation cannot be detected.

To determine experimentally the effect of diffraction losses, which cannot be predicted or measured, on loss tangents, measurements were made with different plate spacings. As plate separation is increased, diffraction losses should also increase and loss tangent values at these plate separations should be larger. Comparing the results obtained and shown in table III indicates that diffraction loss variations with plate separations are small, and the assumption of the same diffraction losses with and without the dielectric slabs between the reflectors seems to be valid. Also diffractions from the edges of the dielectric sheet and frames should also be negligible.

To determine the variations of ϵ and $\tan \delta$ with frequency, measurements were made at different frequencies and the results are shown in table IV. Using data available at lower frequencies (refs. 3 to 5) in addition to those obtained in this investigation, plots of dielectric constant and loss tangent against frequency are shown in figures 13 to 15. The transition region theoretically predicted in figure 1 occurs in the microwave region and continues into the millimeter region. The results of this investigation verified that as the 60 to 90 GHz region is approached, the predicted transition has been passed, and the values of dielectric constants and loss tangent for all frequencies from E-band (60 to 90 GHz) up to but not including the infrared region should be nearly constant.

The dielectric constant for dipole substances is a function of temperature. (See ref. 14.) The variation of dielectric constant of solids with temperature cannot be predicted. Dielectric constant measurements were made by heating the dielectric slabs only, and the results are shown in table V. Plots of dielectric constant against temperature for each material are shown in figure 16. A reduction of dielectric constant at higher temperatures is indicated, although this reduction may not be true in all temperature ranges or for other material.

CONCLUDING REMARKS

The Fabry-Perot interferometer has been demonstrated to be a useful device for measurements of dielectric constants and loss tangents in the millimeter region with

possible application in the submillimeter region. Two methods for making dielectric constant measurements were used and the results obtained from each were comparable; thus, their validity could be verified. For each material, regardless of slab thickness (teflon (1.022 to 2.087), polystyrene (0.985 to 2.010), and lucite (0.123 to 0.372)) and surface finishes (teflon ($\sqrt{16}$ to $\sqrt{32}$), polystyrene ($\sqrt{32}$ to $\sqrt{130}$), and lucite ($\sqrt{8}$)) used in this investigation, the dielectric constants and loss tangents were within 1 percent and ±15 percent, respectively.

Data in the 60 to 90 GHz region which had not been previously available were obtained. The results of this investigation along with existing data at lower frequencies were used to verify the theoretically predicted transition which occurs in the microwave region and continues into the millimeter region. Dielectric constants and loss tangents for teflon, polystyrene, and lucite for all frequencies from E-band (60 to 90 GHz) up to but not including the infrared region should be constant.

Within the temperature range used in this investigation, a reduction of the values of dielectric constant seems to occur at higher temperatures, although this trend may not be true at other temperature ranges or for other materials.

Langley Research Center,
National Aeronautics and Space Administration,
Langley Station, Hampton, Va., October 10, 1969.

APPENDIX A

INTERFEROMETER THEORY AND DERIVATIONS

Impedance Transformation Method

The resonant cavity with the dielectric slab between its plates is shown in figure 7(a). If plane waves and a lossless medium ($\alpha = 0$) between the plates are assumed, the fields in the various regions can be expressed

For region 1 ($0 \leqq x \leqq x_1$):

$$\left.\begin{aligned} E_o &= A_o e^{j(\omega t-\beta x)} + B_o e^{j(\omega t+\beta x)} \\ H_o &= \frac{1}{Z_o}\left[A_o e^{j(\omega t-\beta x)} - B_o e^{j(\omega t+\beta x)}\right] \end{aligned}\right\} \tag{11}$$

For region 2 ($x_1 \leqq x \leqq x_2$):

$$\left.\begin{aligned} E_1 &= A_1 e^{j(\omega t-\beta_1 x)} + B_1 e^{j(\omega t+\beta_1 x)} \\ H_1 &= \frac{1}{Z_1}\left[A_1 e^{j(\omega t-\beta_1 x)} - B_1 e^{j(\omega t+\beta_1 x)}\right] \end{aligned}\right\} \tag{12}$$

For region 3 ($x_2 \leqq x \leqq x_3$):

$$\left.\begin{aligned} E_2 &= A_2 e^{j(\omega t-\beta x)} + B_2 e^{j(\omega t+\beta x)} \\ H_2 &= \frac{1}{Z_o}\left[A_2 e^{j(\omega t-\beta x)} - B_2 e^{j(\omega t+\beta x)}\right] \end{aligned}\right\} \tag{13}$$

where Z_o and Z_1 are the intrinsic impedances in their respective regions defined as

$$Z_o = \left(\frac{\mu_o}{\epsilon_o}\right)^{1/2} \tag{14}$$

$$Z_1 = \left(\frac{\mu_1}{\epsilon_1}\right)^{1/2} \tag{15}$$

APPENDIX A

The standing wave equations for each region can be written

For region 1 $(0 \leqq x \leqq x_1)$:

$$\left.\begin{aligned} E_o &= (A_o + B_o)\cos \beta x - j(A_o - B_o)\sin \beta x \\ H_o &= \frac{1}{Z_o}\left[(A_o - B_o)\cos \beta x - j(A_o + B_o)\sin \beta x\right] \end{aligned}\right\} \tag{16}$$

For region 2 $(x_1 \leqq x \leqq x_2)$:

$$\left.\begin{aligned} E_1 &= (A_1 + B_1)\cos \beta_1 x - j(A_1 - B_1)\sin \beta_1 x \\ H_1 &= \frac{1}{Z_1}\left[(A_1 - B_1)\cos \beta_1 x - j(A_1 + B_1)\sin \beta_1 x\right] \end{aligned}\right\} \tag{17}$$

For region 3 $(x_2 \leqq x \leqq x_3)$:

$$\left.\begin{aligned} E_2 &= (A_2 + B_2)\cos \beta x - j(A_2 - B_2)\sin \beta x \\ H_2 &= \frac{1}{Z_o}\left[(A_2 - B_2)\cos \beta x - j(A_2 + B_2)\sin \beta x\right] \end{aligned}\right\} \tag{18}$$

For resonance, an electric-field node or a magnetic-field antinode must exist at $x = 0$ and $x = x_4 = n\pi$. Therefore, $B_o = -A_o$ and $B_2 = -A_2$. Equations (16), (17), and (18) can then be expressed

For region 1 $(0 \leqq x \leqq x_1)$:

$$\left.\begin{aligned} E_o &= -2jA_o \sin \beta x \\ H_o &= \frac{1}{Z_o}(2A_o \cos \beta x) \end{aligned}\right\} \tag{19}$$

For region 2 $(x_1 \leqq x \leqq x_2)$:

$$\left.\begin{aligned} E_1 &= -2jA_1 \sin \beta_1 x \\ H_1 &= \frac{1}{Z_1}(2A_1 \cos \beta_1 x) \end{aligned}\right\} \tag{20}$$

APPENDIX A

For region 3 $(x_2 \leqq x \leqq x_3)$:

$$\left.\begin{aligned} E_2 &= -2jA_2 \sin \beta x \\ H_2 &= \frac{1}{Z_o}(2A_2 \cos \beta x) \end{aligned}\right\} \tag{21}$$

These equations represent the fields in their respective regions during resonance.

The impedance seen at point x_1, looking toward reflector 1, is given by

$$Z_2 = Z_o \frac{Z_L + jZ_o \tan \beta x_1}{Z_o + jZ_L \tan \beta x_1} \tag{22}$$

By assuming an ideal short at reflector 1, equation (22) is expressed as

$$Z_2 = jZ_o \tan \beta x_1 \tag{23}$$

Such an assumption is valid because plates with reflection coefficients of 0.995 and better can be constructed. At $x = x_2$, the impedance Z_3 is given by

$$Z_3 = Z_1 \frac{Z_2 + jZ_1 \tan \beta_1 s_1}{Z_1 + jZ_2 \tan \beta_1 s_1} \tag{24}$$

and at $x = x_3$, Z_4 is expressed by

$$Z_4 = Z_o \frac{Z_3 + jZ_o \tan \beta s_2}{Z_o + jZ_3 \tan \beta s_2} \tag{25}$$

For interferometer resonance, an electric field node must exist at $x = x_3$; that is, Z_4 must equal zero. Equation (25) can then be expressed as

$$Z_3 + jZ_o \tan \beta s_2 = 0 \tag{26}$$

Substituting equation (23) into equation (24) gives

$$Z_3 = jZ_1 \frac{Z_o \tan \beta x_1 + Z_1 \tan \beta_1 s_1}{Z_1 - Z_o \tan \beta x_1 \tan \beta_1 s_1} \tag{27}$$

Equation (27) can now be inserted into equation (26), and the equation defining resonance is given by

$$\frac{Z_o}{Z_1} \cot \beta_1 s_1 (\cot \beta s_2 + \cot \beta x_1) + \cot \beta x_1 \cot \beta s_2 - \left(\frac{Z_o}{Z_1}\right)^2 = 0 \tag{28}$$

APPENDIX A

By defining $Z_o/Z_1 = k$, equation (28) can be expressed as

$$k(\cot \beta_1 s_1)(\cot \beta s_2 + \cot \beta x_1) + \cot \beta x_1 \cot \beta s_2 - k^2 = 0 \tag{29}$$

By direct measurement of the relative distances between the slab and the plates and slab thickness, the value of k can be found by using equation (29). The expression defining k is given by

$$k = \frac{Z_o}{Z_1} = \left(\frac{\mu_o/\epsilon_o}{\mu_1/\epsilon_1}\right)^{1/2} = \left(\frac{\mu_o \epsilon_1}{\mu_1 \epsilon_o}\right)^{1/2} \tag{30}$$

Since for most nonferrous materials $\mu_o \approx \mu_1$ (the derived equations will not apply for highly conductive slabs), equation (30) can be expressed as

$$k = \left(\frac{\epsilon_1}{\epsilon_o}\right)^{1/2} = (\epsilon)^{1/2} \tag{31}$$

If k is known, the dielectric constant ϵ can be found. It should be noted that equation (29) is a transcendental equation and many values of k will satisfy it.

Dielectric Constant Determination

Once a resonance has been achieved, the insertion of a dielectric will alter the resonant length of the cavity, and a shift in position of one of the reflectors is needed to restore resonance. The dashed plate of figure 7(b) represents the position of plate 2 for resonance before the insertion of the dielectric, and the solid plate, its position for resonance after the insertion of the dielectric.

Before the insertion of the dielectric, $x = 0$ and $x = x_4$ are electric field nodes; therefore,

$$x_1 + s_3 = x_4 = \frac{n\pi}{\beta} \qquad (n = 1, 2, 3, \ldots) \tag{32}$$

Substitution of equation (32) into equation (29) results in

$$k \cot \beta_1 s_1(\cot \beta s_3 - \cot \beta s_2) + \cot \beta s_3 \cot \beta s_2 + k^2 = 0 \tag{33}$$

If Δ is the shift of plate 2 necessary to restore resonance, then

$$s_2 = s_3 - (s_1 + \Delta) \tag{34}$$

Substitution of equation (34) into equation (33) yields

APPENDIX A

$$k \cot \beta_1 s_1 \left\{ \cot \beta s_3 - \cot \beta \left[s_3 - (s_1 + \Delta) \right] \right\} + \cot \beta s_3 \cot \beta \left[s_3 - (s_1 + \Delta) \right] + k^2 = 0 \tag{35}$$

By using equation (35), a curve of Δ against s_3 can be drawn. It has been shown (ref. 13) that the turning points of this curve are given by

$$\tan \beta s_3 = \frac{1}{k} \tan\left(\frac{1}{2} \beta_1 s_1\right) \tag{36}$$

and

$$\tan \beta s_3 = -\frac{1}{k} \cot\left(\frac{1}{2} \beta_1 s_1\right) \tag{37}$$

and the corresponding values of Δ by

$$\tan \frac{1}{2} \beta (s_1 + \Delta) = \frac{1}{k} \tan\left(\frac{1}{2} \beta_1 s_1\right) \tag{38}$$

$$\tan \frac{1}{2} \beta (s_1 + \Delta) = k \tan\left(\frac{1}{2} \beta_1 s_1\right) \tag{39}$$

The sign of $\tan \frac{\beta_1 s_1}{2}$ determines which of equations (38) or (39) represents Δ_{max} or Δ_{min}. Since $k > 1$, it is evident that when the integral part of $2s_1/\lambda_1$ is zero or an even integer, equation (38) gives Δ_{min} and equation (39) gives Δ_{max}; when the integral part of $2s_1/\lambda_1$ is an odd integer, equation (38) gives Δ_{max} and equation (39) gives Δ_{min}.

Another form of equation (35) is given by

$$\tan \beta (s_1 + \Delta) = \tan \beta_1 s_1 \frac{\cot \beta s_3 + k^2 \tan \beta s_3}{k(\tan \beta s_3 + \cot \beta s_3) + (k^2 - 1) \tan \beta_1 s_1} \tag{40}$$

When the thickness of the dielectric slab is an integral number of half-wavelengths, or

$$\beta_1 s_1 = n\pi = \frac{n\lambda}{2} \qquad (n = 1, 2, 3, \ldots) \tag{41}$$

equation (40) is equal to

$$\left.\begin{aligned} &\tan \beta (s_1 + \Delta) = \tan \beta_1 s_1 = 0 \\ &\beta (s_1 + \Delta) = \beta_1 s_1 = n\pi \\ &\Delta = s_1 (k - 1) \end{aligned}\right\} \tag{42}$$

APPENDIX A

By examining equation (29), which describes the interferometer resonance when the dielectric slab is between the plates, it can be concluded that there is a linear relation between x_1 and s_2 when the dielectric thickness is a multiple of half-wavelength. Such a relation is given by

$$\left.\begin{aligned} &\cot \beta s_2 = -\cot \beta x_1 \\ &\beta s_2 = -\beta x_1 + n\pi \qquad (n = 0, \pm 1, \pm 2, \ldots) \\ &x_1 + s_2 = \frac{n\lambda}{2} \qquad (n = 0, \pm 1, \pm 2, \ldots) \end{aligned}\right\} \tag{43}$$

Thus, when $\beta_1 s_1 = n\pi$, the condition for resonance depends on the sum of the distances s_2 and x_1, as given by equation (43). Once resonance has been restored after the insertion of the slab, a change in the position of the slab will not disturb resonance, as long as equations (41) and (43) are satisfied. This fact can better be understood by remembering, from impedance transformation techniques, that layers of multiples of half-wavelengths thick produce no change in the impedance seen before and after them. Thus, the Δ required to restore resonance will be the same for any position of the dielectric.

Therefore, there is evidence that there are at least three possible methods of determining the dielectric constant of a slab. (See ref. 5.) The first and most direct method would be to use equation (29). By directly measuring distances x_1, s_1, and s_2 and knowing the operating wavelength, the value of k can be found.

A second method is to plot Δ against s_3 for each dielectric slab. The values of Δ will oscillate between Δ_{max} and Δ_{min} as a function of s_3. Once Δ_{max} and Δ_{min} have been determined, k can be found by using equations (38) and (39). A computer program is recommended for determining k by this method.

The third method would be to use slabs whose thicknesses are multiples of half-wavelengths. By measuring Δ, the shift of the position of plate 2 to restore resonance, k can be determined from equation (42). This method probably would be the easiest method for determining k if one varies the frequency to obtain an integral number of half-wavelengths in the slab to be measured.

Loss Tangent Evaluation

Most resonators are usually judged by their quality factor Q which is defined as

$$Q = \omega \frac{\text{Energy stored}}{\text{Mean dissipation of power}} \tag{44}$$

The average power loss or the dissipated power in the cavity is given by

$$P_s = \frac{R(s)}{2} \iint_{\text{Cavity walls}} H_{tan} \cdot H_{tan}^* \, dS \tag{45}$$

where $R(s)$ is the real part of the surface impedance of the plates, and H_{tan} is the magnetic field tangential to the plate surfaces. The maximum stored energy W_s in a cavity resonator of any arbitrary shape for a sinusoidally time-varying field is given by

$$W_s = \frac{\epsilon_1}{2} \iiint_V E \cdot E^* \, dV = \frac{\mu_1}{2} \iiint_V H \cdot H^* \, dV \tag{46}$$

where V denotes the volume of the cavity. Thus, if the field distribution inside the cavity is known, Q and the resonant frequency can be determined. The field distribution for many shapes of cavities is difficult to determine. However, for some simple geometrical shapes of a cavity, it is possible to estimate the field distribution, and hence determine Q and the resonant frequency fairly accurately. Since the dimensions of the cavity are such that higher modes, other than the TEM mode, do not exist inside the cavity, the equations derived previously in each region can now be used to derive the Q of the cavity with and without the dielectric. By assuming that there is a lossless medium between the plates, the energy stored is given by

$$\left.\begin{aligned} W_s &= \frac{\epsilon_o}{2} \iiint E_o \cdot E_o^* \, dV \\ W_s &= \frac{\epsilon_o}{2} \int_V \iint 4A_o^2 \sin^2 \beta x \, dV \end{aligned}\right\} \tag{47}$$

If it is remembered that for resonance $d = n\pi$, equation (47) can be written as

$$W_s = \epsilon_o \, dA_o^2 \int_A \int dS \tag{48}$$

The average power loss or the dissipated power in the cavity per plate is given by

$$\left.\begin{aligned} P_s &= \frac{R(s)}{2} \iint H_{tan} \cdot H_{tan}^* \, dS \\ P_s &= \frac{2A_o^2 R(s)}{Z_o^2} \int_A \int \cos^2 \beta x \, dS \end{aligned}\right\} \tag{49}$$

Since the surfaces of the reflector plates at resonance are at distances equal to $x = 0$ and $x = n\pi$, equation (49) can be written as

$$P_s = \frac{2A_o^2 R(s)}{Z_o^2} \int_A \int dS \tag{50}$$

APPENDIX A

Equation (50) represents losses per plate. By assuming that the losses in both plates are equal, the total dissipated power in the plates is given by

$$P_s = \frac{4A_o^2 R(s)}{Z_o^2} \int_A \int dS \tag{51}$$

By using the basic definition given by equation (44) and substituting equations (48) and (51), Q_o is represented by

$$Q_o = \frac{\omega \epsilon_o d}{4R(s)/Z_o^2} \tag{52}$$

Equation (52) represents the Q_o of the cavity when there are no diffraction losses from the sides of the interferometer. The evaluation of Q is simplified (ref. 5) by assuming that the diffraction losses with and without the dielectric are the same, and that slabs whose thicknesses are multiples of half-wavelengths are used.

To account for diffraction losses, an additional term P_d is added in equation (52), and thus Q_o without the dielectric may be expressed as

$$Q_o = \frac{\omega \epsilon_o d}{\frac{4R(s)}{Z_o^2 + P_d}} \tag{53}$$

The radiation resistance of the cavity due to transmission through the end plates is also included in P_d. Once the dielectric is inserted between the plates, Q of the cavity is reduced and is given by

$$Q = \frac{\omega\left(\frac{\epsilon_o}{2}\int_A dS \int_0^{x_1} |E_o|^2 dx + \frac{\epsilon'}{2}\int_A dS \int_{x_1}^{x_2} |E_1|^2 dx + \frac{\epsilon_o}{2}\int_A ds \int_{x_2}^{x_3} |E_2|^2 dx\right)}{\frac{\omega\epsilon''}{2}\int_A dS \int_{x_1}^{x_2} |E_1|^2 dx + \frac{R(s)}{2}\int_A |H_o|^2 dS + \frac{R(s)}{2}\int_A |H_2|^2 dS + P_d A_o \int_A ds} \tag{54}$$

The evaluation of equation (54) using the expression for the fields derived previously is very complicated. If sheets whose thicknesses are multiples of half-wavelengths are available, equation (54) is given by

$$Q_t = \frac{\omega\left[\epsilon_o A_o^2 (x_1 + s_2) + \epsilon' s_1 A_o^2 \left(k^{-2}\cos^2\beta_1 x_1 + \sin^2\beta_1 x_1\right)\right]}{\omega\epsilon'' s_1 A_o^2 \left(k^{-2}\cos^2\beta_1 x_1 + \sin^2\beta_1 x_1\right) + \frac{4A_o^2 R(s)}{Z_o^2} + P_d A_o^2} \tag{55}$$

where $\epsilon = \epsilon' - j\epsilon''$ is the complex dielectric constant and $\tan \delta = \frac{\epsilon''}{\epsilon'}$. By assuming that dielectric losses exceed resistive and diffraction losses, the maximum value of equation (55) occurs when $\beta x_1 = n\pi$ and is given by

$$\frac{1}{Q_{t,max}} = \frac{1}{Q_o} + \frac{s_1}{d} \tan \delta \tag{56}$$

where $d = x_1 + s_1 + s_2$.

APPENDIX B

FABRY-PEROT INTERFEROMETER

Resonant Cavity

The basic structure of a flat-plate Fabry-Perot resonant cavity is shown in figure 17. The Q (quality factor) of the cavity is a function of plate separation, diffraction losses, and reflection losses. The sidewall losses which are present in cavities of lower microwave frequencies have been eliminated by the absence of any sidewalls. However, diffraction losses have been introduced which result from the finite aperture of the reflector plates and from the imperfection in their flatness, and they can be controlled by the use of the appropriate size plates and plate separation. Any misalinement of the plates from parallelism will increase diffraction losses and reduce Q. Reflection losses are present because of the absorption in the reflector plates and transmission through them.

The Q of the Fabry-Perot resonator (ref. 9) is given

$$Q = \frac{2\pi d}{\gamma\lambda} \tag{57}$$

where

d distance between reflecting plates

λ operating wavelength

γ sum of reflection and diffraction losses

It would seem valid that for a given value of reflection and diffraction losses, Q would vary linearly with plate separation. Since reflection and diffraction losses are functions of plate separation, at some point the combination of the two would be such that a maximum Q is achieved. As the plate separation is increased beyond that point, the value of Q will begin to decrease. Figure 18 demonstrates how the theoretical and experimental values of Q vary. There should be a linear relation up to a certain point which will indicate that the sum of diffraction and reflection losses is approximately constant. As the plate separation is increased further, the sum of the diffraction and reflection losses does not stay constant, and, as a result, there is a bending of the curve.

When a dielectric is inserted between the plates, additional losses are introduced. The propagation losses through the medium, which vary as the thickness, must be accounted for. Thus, an additional term must be added in deciding on the value of γ.

It must also be remembered that additional diffraction losses could result from the imperfections of the dielectric sample.

Operating Principle

The resonant cavity which was introduced previously can be thought of as being an interference light filter (ref. 15) which is used extensively in the field of optics. When the plate separation is an integral number of a half-wavelength ($d = \lambda/2,\ \lambda,\ 3\lambda/2,\ \ldots$), complete reflection occurs, and electric field intensity at the boundary will be zero, if it is assumed that the reflecting surface is a perfect conductor. Hence, the metallic surface of the reflecting plate will absorb no energy from the electromagnetic wave. Practically, such a surface cannot be constructed, but surfaces with reflection coefficients close to unity can be achieved. Since an ideal electric field node cannot be attained, wave absorption in the light filter is due to the ohmic losses of currents induced in the metallic surfaces.

When the plate separation is equal to an odd number of a quarter-wavelength ($d = \lambda/4,\ 3\lambda/4,\ 5\lambda/4,\ \ldots$), minimum reflection will occur. If the metallic surface of one reflecting plate is located at a node of the electric field, the surface of the other reflecting plate will be at an antinode, and the absorption of the electromagnetic wave by the plates of the light filter will be maximum. The transmission through the light filter can be verified mathematically by considering the resonant cavity of the interferometer (fig. 19) and applying the principle of multiple reflections by assuming plane waves.

For simplification of notation, it is assumed that the transmission coefficients $t_{12} = t_{21} = t_{32} = t_o$ and reflection coefficients $\rho_1 = \rho_2 = \rho_3 = \rho_o$. The principle of operation is the same and is best illustrated by the more simplified notation. The fields in the various regions can then be calculated. Thus, in region 1 the field E_1 can be expressed by

$$E_1 = E_o\rho_o + E_o t_o^2 \rho_o e^{-j2\beta d} + E_o t_o^2 \rho_o^3 e^{-j4\beta d} + E_o t_o^2 \rho_o^5 e^{-j6\beta d} + \ldots$$

$$E_1 = \rho_o E_o\left[1 + t_o^2 e^{-j2\beta d}\left(1 + \rho_o^2 e^{-j2\beta d} + \rho_o^4 e^{-j4\beta d} + \ldots\right)\right]$$

$$E_1 = \rho_o E_o\left[1 + t_o^2 e^{-j2\beta d}\left(\frac{1}{1 - \rho_o^2\, e^{-j2\beta d}}\right)\right]$$

$$\frac{E_1}{E_o} = \frac{\rho_o\left[1 + \left(t_o^2 - \rho_o^2\right)e^{-j2\beta d}\right]}{1 - \rho_o^2 e^{-j2\beta d}} \tag{58}$$

APPENDIX B

The ratio of (E_1/E_o) defines the total reflection coefficient of the resonant cavity. Similarly, the field in region 2 is found to be

$$E_2 = E_o t_o e^{-j\beta x} + E_o t_o \rho_o e^{-j\beta(2d-x)} + E_o t_o \rho_o^2 e^{-j\beta(2d+x)}$$

$$+ E_o t_o \rho_o^3 e^{-j\beta(4d-x)} + E_o t_o \rho_o^4 e^{-j\beta(4d+x)}$$

$$E_2 = E_o t_o e^{-j\beta x}\left[1 + \rho_o e^{-j2\beta(d-x)} + \rho_o^2 e^{-j2\beta d} + \rho_o^3 e^{-j2\beta(2d-x)} + \ldots\right]$$

$$E_2 = E_o t_o e^{-j\beta x}\left[1 + \rho_o e^{-j2\beta(d-x)}\right]\left[1 + \rho_o^2 e^{-j2\beta d} + \rho_o^4 e^{-j4\beta d} + \ldots\right]$$

$$\frac{E_2}{E_o} = \frac{t_o e^{-j\beta x}\left[1 + \rho_o e^{-j2\beta(d-x)}\right]}{1 - \rho_o^2 e^{-j2\beta d}} \tag{59}$$

The field in region 3 is given by

$$E_3 = E_o t_o^2 e^{-j\beta d} + E_o t_o^2 \rho_o^2 e^{-j3\beta d} + E_o t_o^2 \rho_o^4 e^{-j5\beta d} + \ldots$$

$$E_3 = E_o t_o^2 e^{-j\beta d}\left(1 + \rho_o^2 e^{-j2\beta d} + \rho_o^4 e^{-j4\beta d} + \ldots\right)$$

$$\frac{E_3}{E_o} = \frac{t_o^2 e^{-j\beta d}}{1 - \rho_o^2 e^{-j2\beta d}} \tag{60}$$

The ratio of $|E_3/E_o|$ defines the transmission coefficient of the entire resonant cavity.

To find the optimum spacing for maximum transmission, equation (60) is differentiated with respect to βd and then set equal to zero. Thus,

$$1 + \rho_o^2 e^{-j2\beta d} = 0$$

$$\beta d = \frac{n\pi}{2} \qquad (n = 1, 2, 3, 4, \ldots) \tag{61}$$

APPENDIX B

Maximum transmission occurs when

$$\beta d = \frac{n\pi}{2} \qquad (n = 2, 4, 6, \ldots) \tag{62}$$

or

$$d = \frac{\lambda}{2}, \ \lambda, \ \frac{3\lambda}{2}, \ \ldots \tag{63}$$

Minimum transmission occurs when

$$\beta d = \frac{n\pi}{2} \qquad (n = 1, 3, 5, \ldots) \tag{64}$$

or

$$d = \frac{\lambda}{4}, \ \frac{3\lambda}{4}, \ \frac{5\lambda}{4}, \ \ldots \tag{65}$$

The magnetic fields in the three regions can be calculated by using the same procedure as for the electric fields, and they are given by

$$H_1 = - \frac{E_o \rho_o \left(1 + e^{-j2\beta d}\right)}{Z_o \left(1 - \rho_o^2 e^{-j2\beta d}\right)} \tag{66}$$

$$H_2 = \frac{E_o t_o e^{-j\beta x} \left[1 - \rho_o e^{-j2\beta(d-x)}\right]}{Z_o \left(1 - \rho_o^2 e^{-j2\beta d}\right)} \tag{67}$$

$$H_3 = \frac{E_o}{Z_o} \frac{t_o^2 e^{-j\beta d}}{1 - \rho_o^2 e^{-j2\beta d}} \tag{68}$$

REFERENCES

1. Dekker, Adrianus J.: Solid State Physics. Prentice-Hall, Inc., 1957.

2. Montgomery, Carol G., ed.: Technique of Microwave Measurements. McGraw-Hill Book Co., Inc., 1947.

3. Von Hippel, Arthur R., ed.: Dielectric Materials and Applications. The Technology Press of M.I.T., c.1954.

4. Hakki, B. W.; and Coleman, P. D.: A Dielectric Resonator Method of Measuring Inductive Capacities in the Millimeter Range. IRE Trans. Microwave Theory and Tech., vol. MTT-8, no. 4, July 1960, pp. 402-410.

5. Culshaw, W.; and Anderson, M. V.: Measurement of Permittivity and Dielectric Loss With a Millimetre-Wave Fabry-Perôt Interferometer. Paper No. 3763E, Inst. Elect. Eng., May 1962, pp. 820-826.

6. Balanis, Constantine A.: Investigation of a Proposed Technique for Measurements of Dielectric Constants and Losses at V-band Using the Fabry-Perot Principle. M.E.E. Thesis, Univ. Virginia, 1966.

7. Breeden, K. H.; and Sheppard, A. P.: Millimeter and Submillimeter Wave Dielectric Measurements. Microwave J., vol. 10, no. 12, Nov. 1967, pp. 59-62.

8. Degenford, J. E.; and Coleman, P. D.: A Quasi-Optics Perturbation Technique for Measuring Dielectric Constants. Proc. IEEE, vol. 54, no. 4, Apr. 1966, pp. 520-522.

9. Boyd, G. D.; and Gordon, J. P.: Confocal Multimode Resonator for Millimeter Through Optical Wavelength Masers. Bell System Tech. J., vol. 40, no. 2, Mar. 1961, pp. 489-508.

10. Culshaw, William: High Resolution Millimeter Wave Fabry-Perot Interferometer. IRE, Trans. Microwave Theory Tech., vol. MTT-8, no. 2, Mar. 1960, pp. 182-189.

11. Culshaw, William: Resonators for Millimeter and Submillimeter Wavelengths. IRE, Trans. Microwave Theory Tech., vol. MTT-9, no. 2, Mar. 1961, pp. 135-144.

12. Zimmerer, R. W.; Anderson, M. V.; Strine, G. L.; and Beers, Y.: Millimeter Wavelength Resonant Structures. IEEE Trans. Microwave Theory Tech., vol. MTT-11, no. 2, Mar. 1963, pp. 142-149.

13. Lamont, H. R. L.: Theory of Resonance in Microwave Transmission Lines With Discontinuous Dielectric. London, Edinburgh & Dublin Phil. Mag. J. Sci., vol. 29, no. 197, June 1940, pp. 521-540.

14. Smyth, Charles Phelps: Dielectric Behavior and Structure. Dielectric Constant and Loss, Dipole Moment and Molecular Structure. McGraw-Hill Book Co., Inc., c.1955.

15. Brekhovskikh, Leonid M. (David Lieberman, trans.): Waves in Layered Media. Academic Press Inc., c.1960.

TABLE I.- DIELECTRIC CONSTANTS FOR VARIOUS MATERIALS OF SEVERAL THICKNESSES AND VARIOUS SURFACE FINISHES AT 25° C USING FIRST METHOD

Thickness		Surface finish	Dielectric constant	Frequency, MHz
in.	mm			
		Teflon		
1.022 ± 0.005	25.959 ± 0.127	32	2.06	61 452
1.092 ± 0.001	27.737 ± 0.025	16	2.05	61 452
1.637 ± 0.001	41.580 ± 0.025	16	2.05	61 452
2.087 ± 0.005	53.010 ± 0.127	32	2.06	61 452
		Polystyrene		
0.985 ± 0.001	25.019 ± 0.025	32	2.53	61 452
1.012 ± 0.002	25.705 ± 0.051	64	2.53	61 452
1.473 ± 0.001	37.414 ± 0.025	32	2.53	61 452
2.010 ± 0.002	51.054 ± 0.051	130	2.53	61 452
		Lucite		
0.123 ± 0.002	3.124 ± 0.051	8	---	
0.183 ± 0.002	4.648 ± 0.051	8	2.59	61 452
0.372 ± 0.003	9.449 ± 0.076	8	2.60	61 452

TABLE II.- DIELECTRIC CONSTANTS FOR VARIOUS MATERIALS OF SEVERAL THICKNESSES AND VARIOUS SURFACE FINISHES AT 25° C USING SECOND METHOD

Thickness		Surface finish	Dielectric constant	Frequency, MHz
in.	mm			
		Teflon		
1.022 ± 0.005	25.959 ± 0.127	32	2.05	60 539
1.092 ± 0.001	27.737 ± 0.025	16	2.06	60 319
1.637 ± 0.001	41.580 ± 0.025	16	2.05	60 449
2.087 ± 0.005	53 010 ± 0.127	32	---	-----
		Polystyrene		
0.985 ± 0.001	25.019 ± 0.025	32	2.53	60 246
1.012 ± 0.002	25.705 ± 0.051	64	2.53	58 677
1.473 ± 0.001	37.414 ± 0.025	32	2.54	60 418
2.010 ± 0.002	51.054 ± 0.051	130	---	-----
		Lucite		
0.123 ± 0.002	3.124 ± 0.051	8	2.58	59 562
0.183 ± 0.002	4.648 ± 0.051	8	2.59	60 065
0.372 ± 0.003	9.449 ± 0.076	8	---	-----

TABLE III.- LOSS TANGENTS FOR VARIOUS MATERIALS OF SEVERAL THICKNESSES AND VARIOUS SURFACE FINISHES AT CONSTANT TEMPERATURE (25° C)

Thickness		Surface finish	Frequency, MHz	tan δ for –		
in.	mm			d ≈ 4.8 in. (121.92 mm)	d ≈ 5.5 in. (139.70 mm)	d ≈ 6.5 in. (165.10 mm)
Teflon						
1.022 ± 0.005	25.959 ± 0.127	$\sqrt{32}$	60 539	2.34×10^{-4}	1.82×10^{-4}	2.15×10^{-4}
1.092 ± 0.001	27.737 ± 0.025	$\sqrt{16}$	60 319	2.39	2.21	2.75
1.637 ± 0.001	41.580 ± 0.025	$\sqrt{16}$	60 449	----------	2.27	3.05
Polystyrene						
0.985 ± 0.001	25.019 ± 0.025	$\sqrt{32}$	60 246	----------	6.98×10^{-4}	7.05×10^{-4}
1.012 ± 0.002	25.705 ± 0.051	$\sqrt{64}$	58 677	----------	9.41	9.72
1.473 ± 0.001	37.414 ± 0.025	$\sqrt{32}$	60 418	----------	7.16	7.15
Lucite						
0.123 ± 0.002	3.124 ± 0.051	$\sqrt{8}$	59 562	----------	59.45×10^{-4}	59.09×10^{-4}
0.183 ± 0.002	4.648 ± 0.051	$\sqrt{8}$	60 065	----------	59.14	58.87

TABLE IV.- DIELECTRIC CONSTANTS AND LOSS TANGENTS FOR VARIOUS MATERIALS AT DIFFERENT FREQUENCIES AND CONSTANT TEMPERATURE (25° C)

Frequency, MHz	tan δ	Dielectric constant
Teflon; s_1 = 1.092 in. (27.737 mm)		
60 319	2.2×10^{-4}	2.06
86 644	2.2	2.06
Polystyrene; s_1 = 1.012 in. (25.705 mm)		
58 677	9.4×10^{-4}	2.53
91 627	11.7	2.53
Lucite; s_1 = 0.123 in. (3.124 mm)		
59 562	59×10^{-4}	2.58
89 709	84	2.56

TABLE V.- DIELECTRIC CONSTANTS OF DIFFERENT MATERIALS FOR VARIOUS TEMPERATURES AND CONSTANT FREQUENCY

Temperature, °C	Frequency, MHz	Dielectric constant for –		
		Teflon; s_1 = 1.092 in. (27.737 mm)	Polystyrene; s_1 = 1.012 in. (25.705 mm)	Lucite; s_1 = 0.123 in. (3.124 mm)
-8	61 242	2.05	2.54	2.63
8	61 242	2.05	2.54	2.61
24	61 242	2.04	2.54	2.60
32	61 242	2.03	2.53	2.57
46	61 242	2.02	2.53	2.58
65	61 242	2.01	2.52	2.57
77	61 242	2.01	2.52	2.55

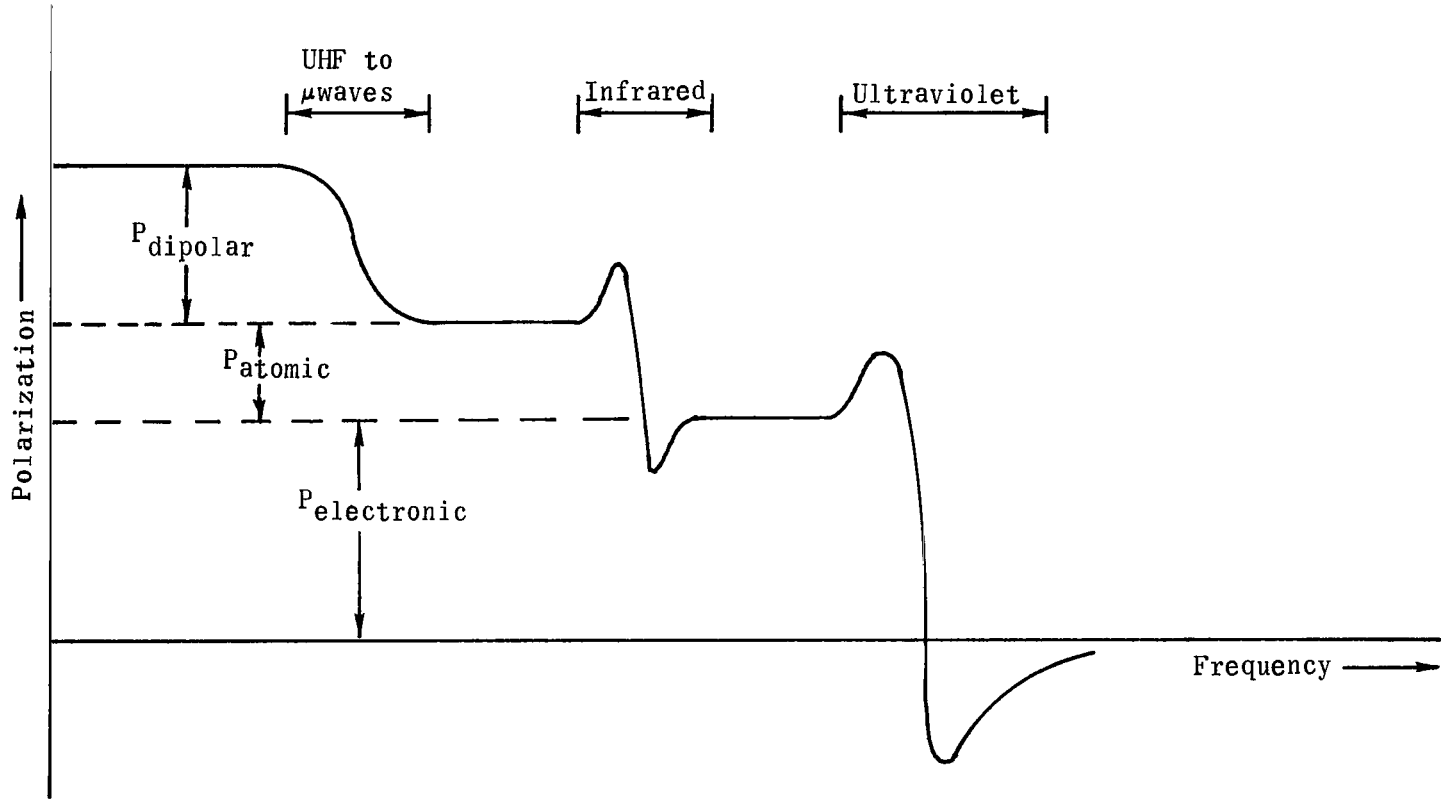

Figure 1.- Real part of total polarization P as function of frequency for a dipolar substance with a single atomic and electronic resonance frequency.

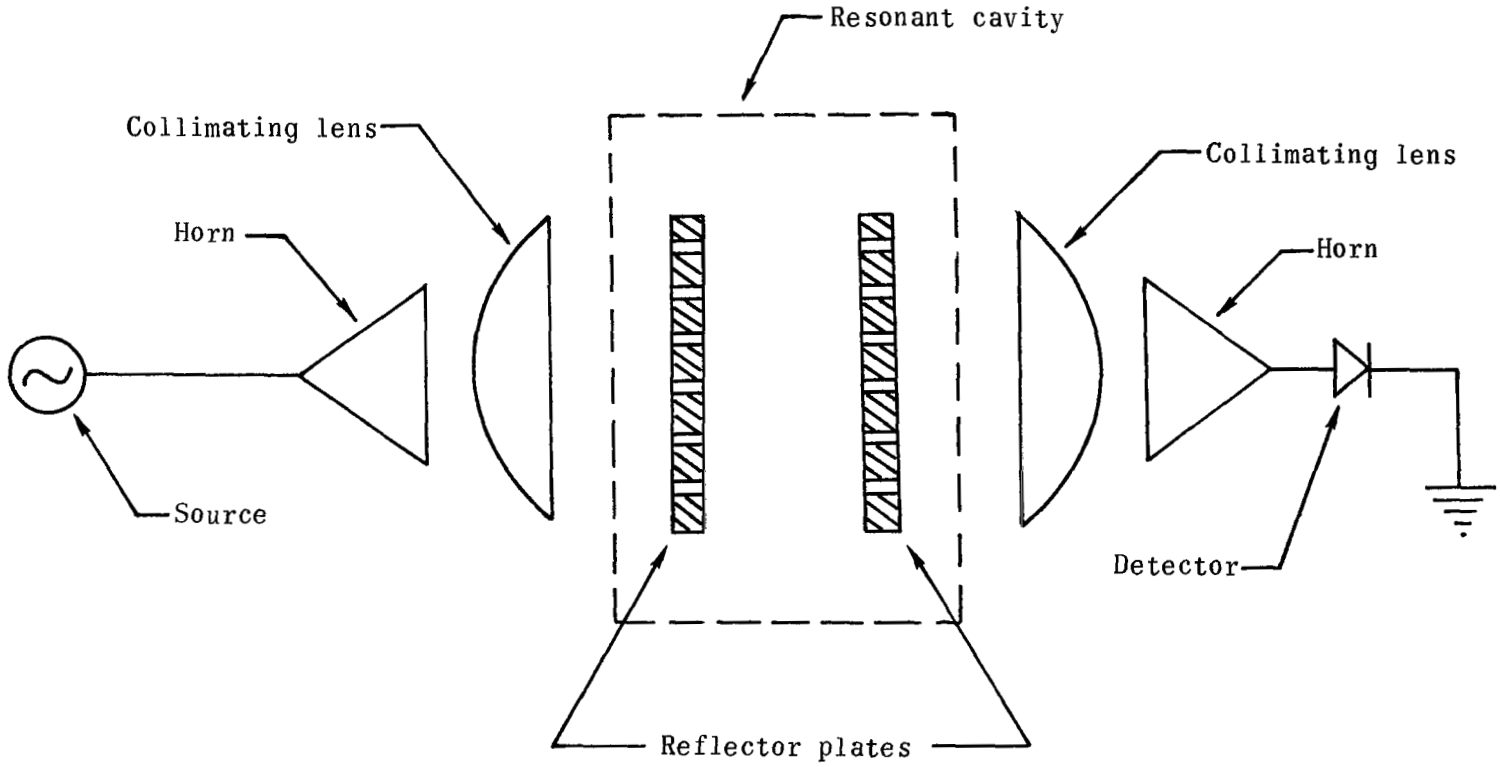

Figure 2.- Flat plate Fabry-Perot interferometer.

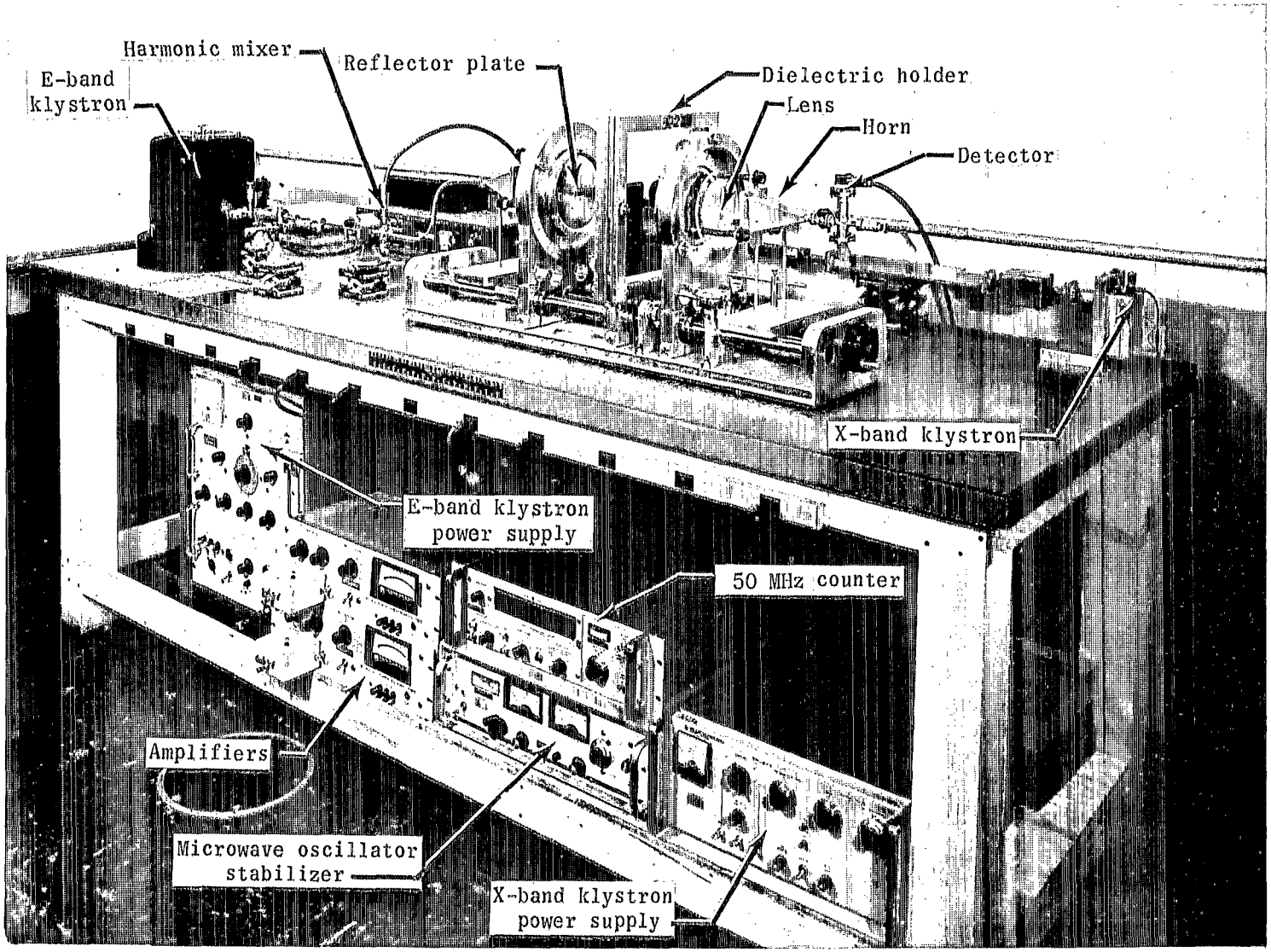

Figure 3.- System used for measurements of dielectric constant and loss tangent at millimeter region.

L-66-2984.1

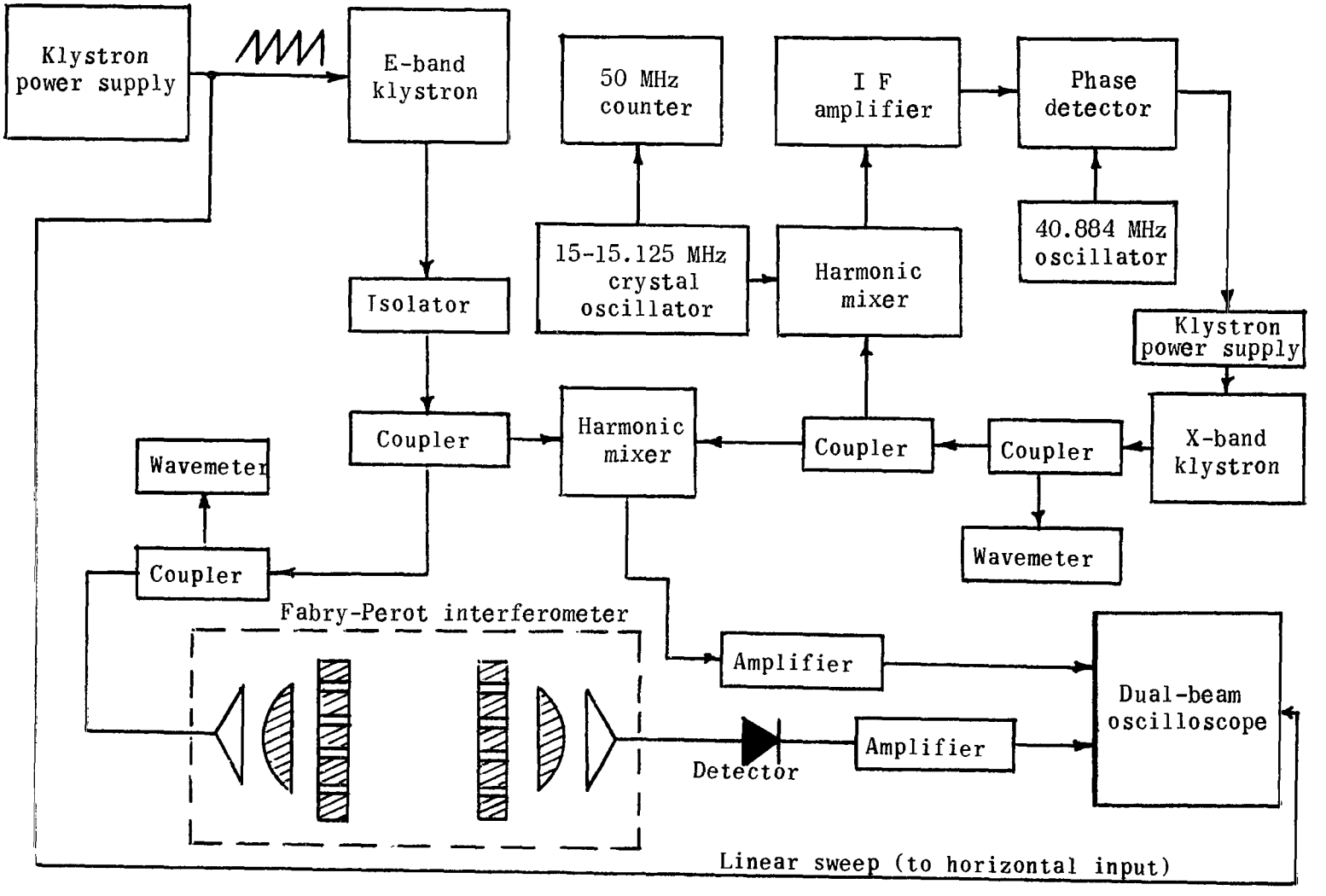

Figure 4.- Block diagram of system for measurement of dielectric constant and loss tangent at millimeter region.

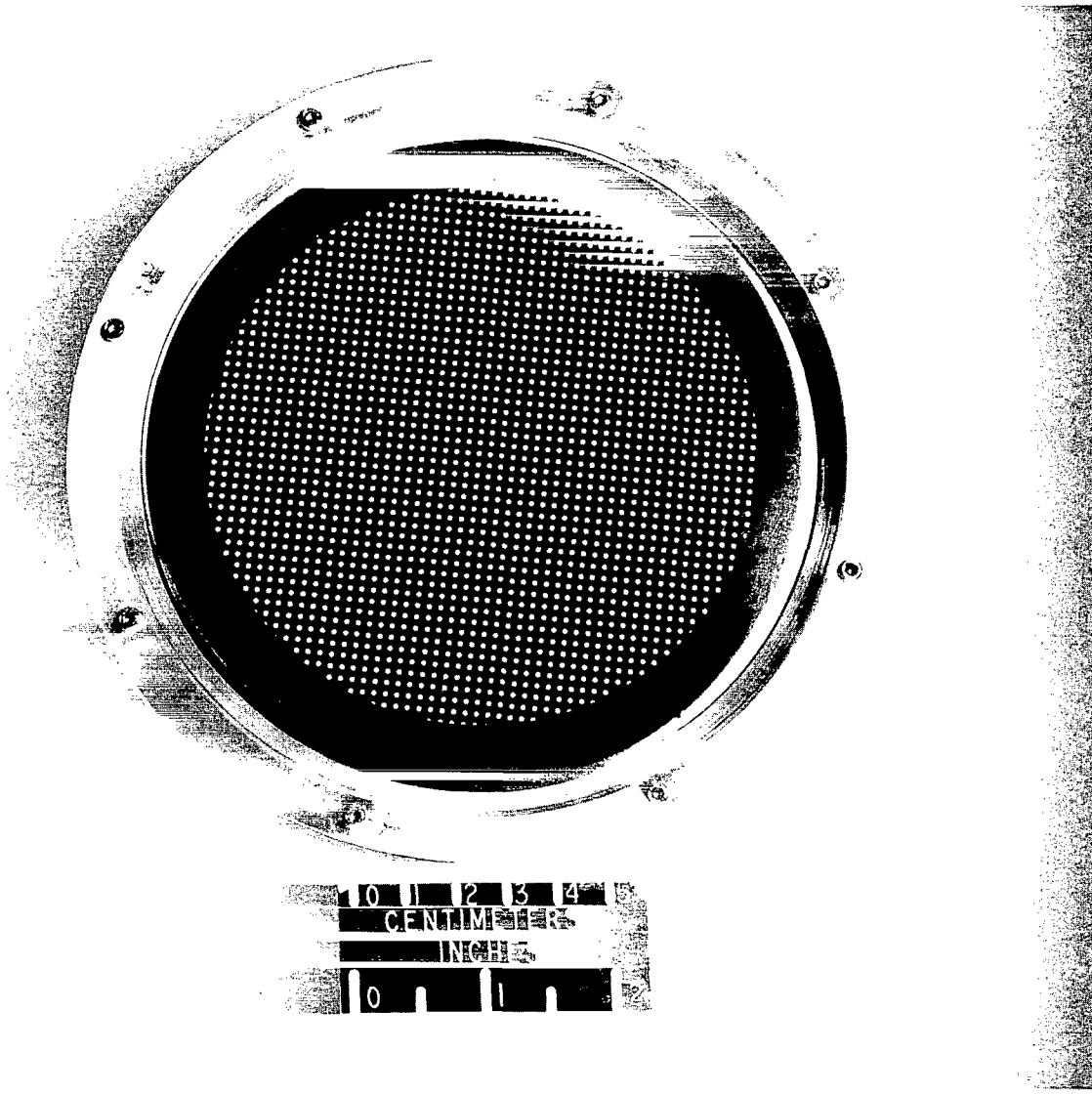

Figure 5.- Perforated reflector plate.

L-66-2979

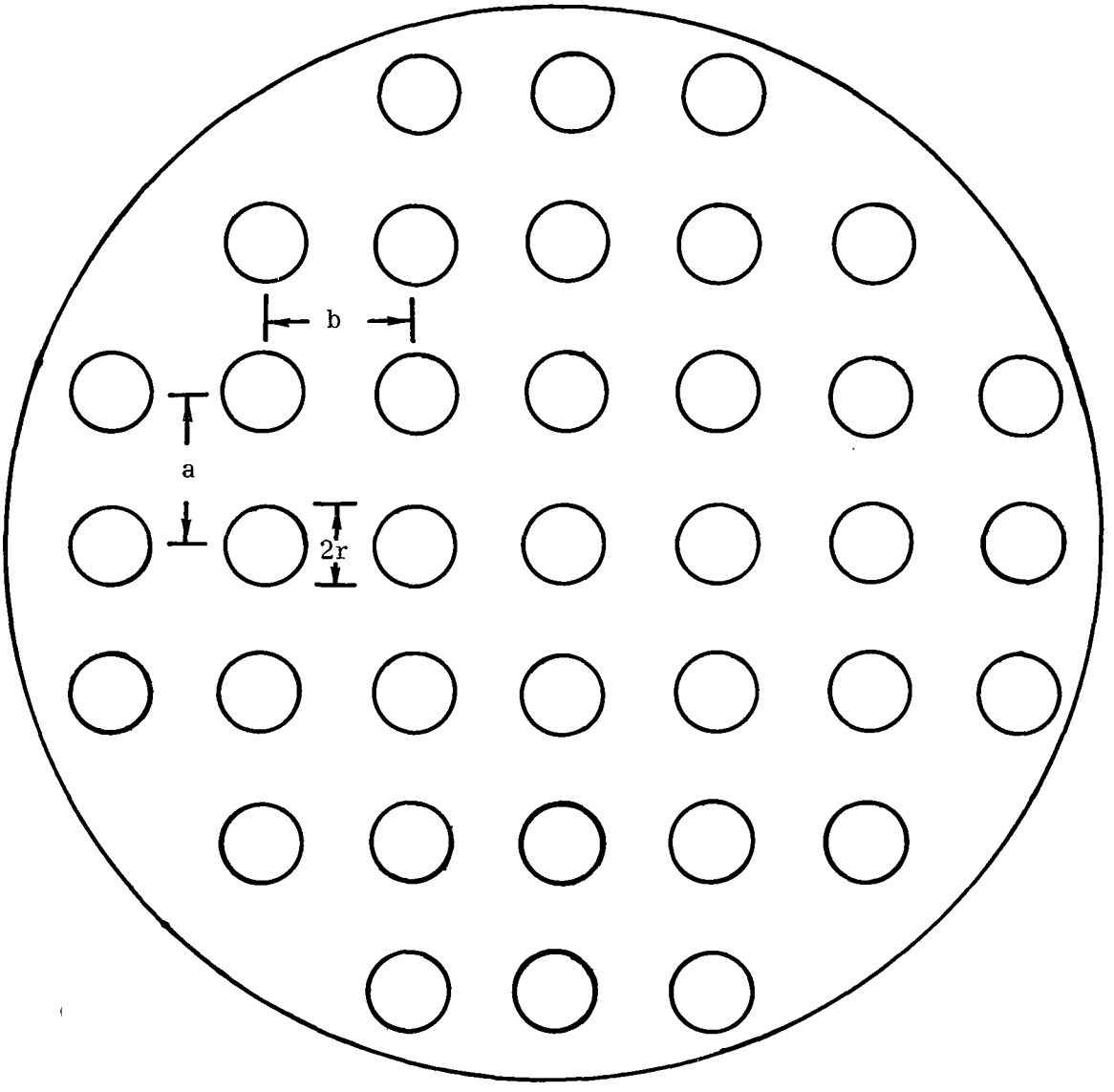

Figure 6.- Hole pattern of reflector plate (a = b = 0.1 inch (2.54 mm), r = 0.02 inch (0.508 mm)).

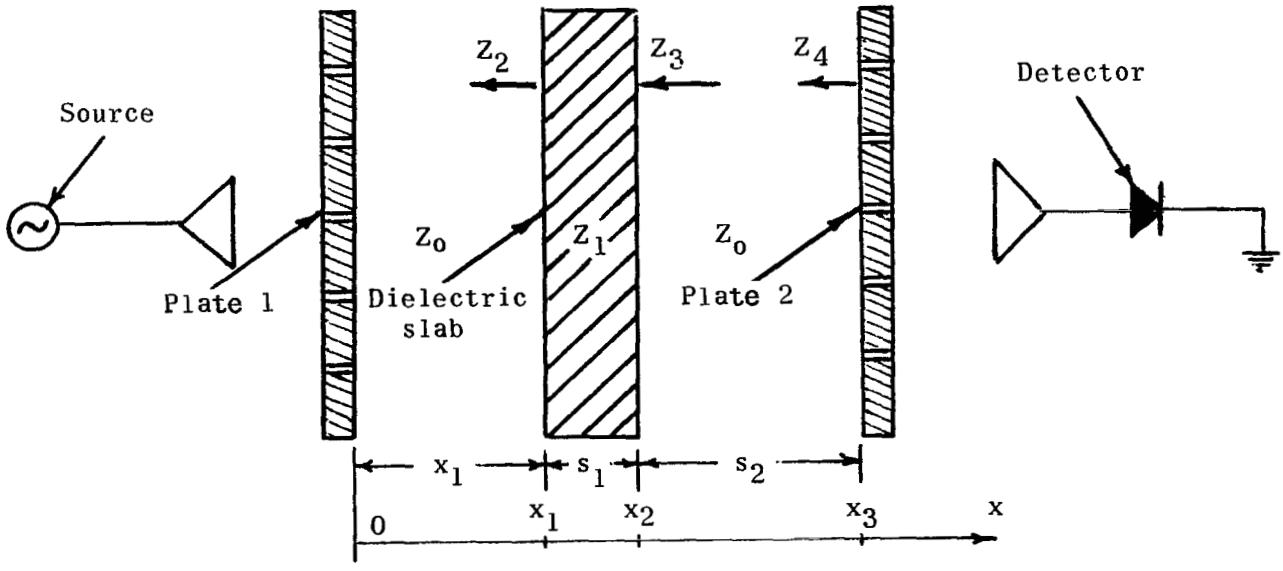

(a) Resonance with dielectric slab.

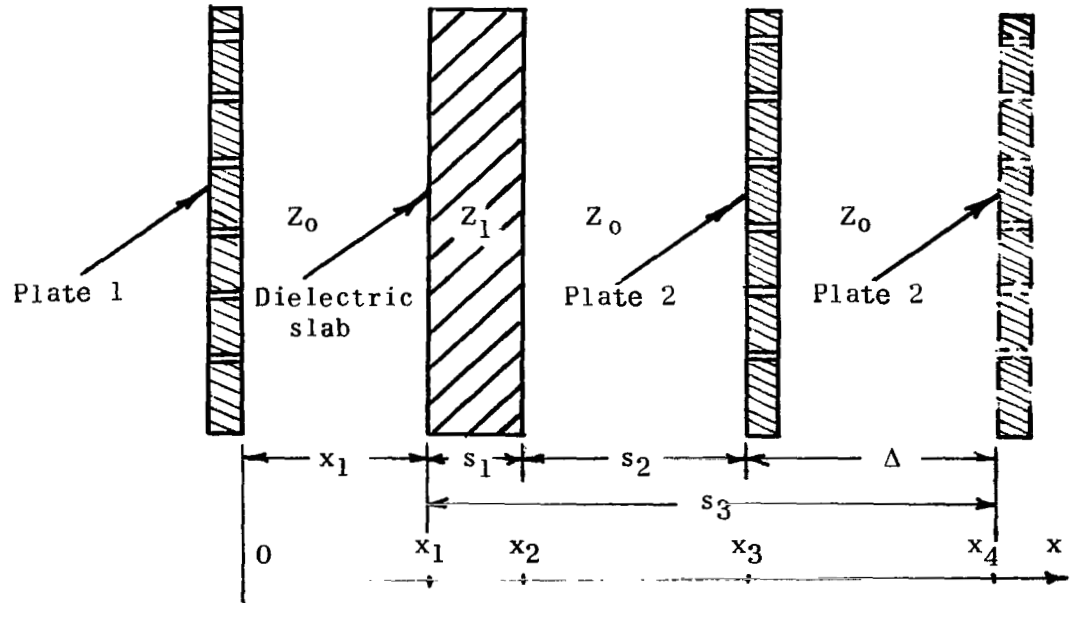

(b) Resonance with and without dielectric slab.

Figure 7.- Relative positions of reflector plates and slab for resonance.

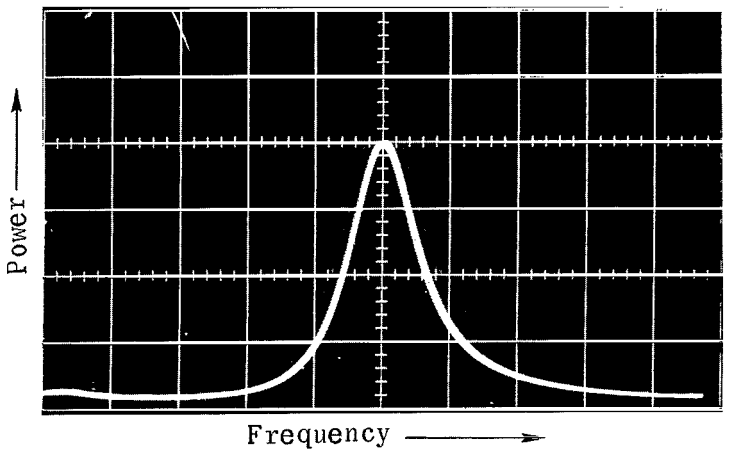

(a) Response with air. Q = 10 960.

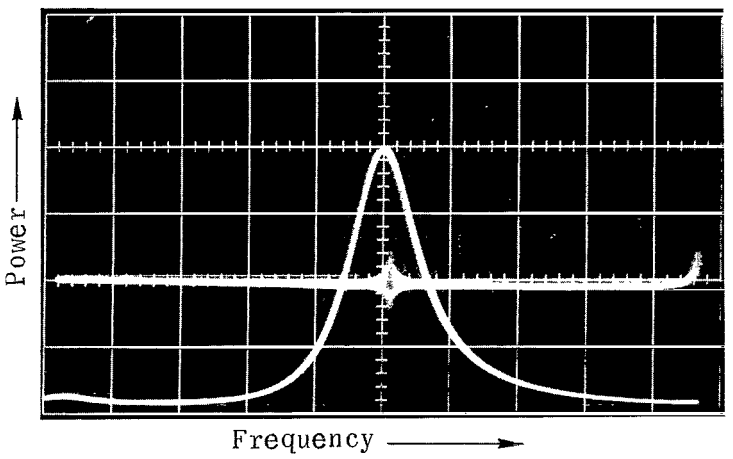

(b) Response and zero beat used as a variable frequency marker. Q = 10 960.

Figure 8.- Cavity response curve and variable-frequency marker.

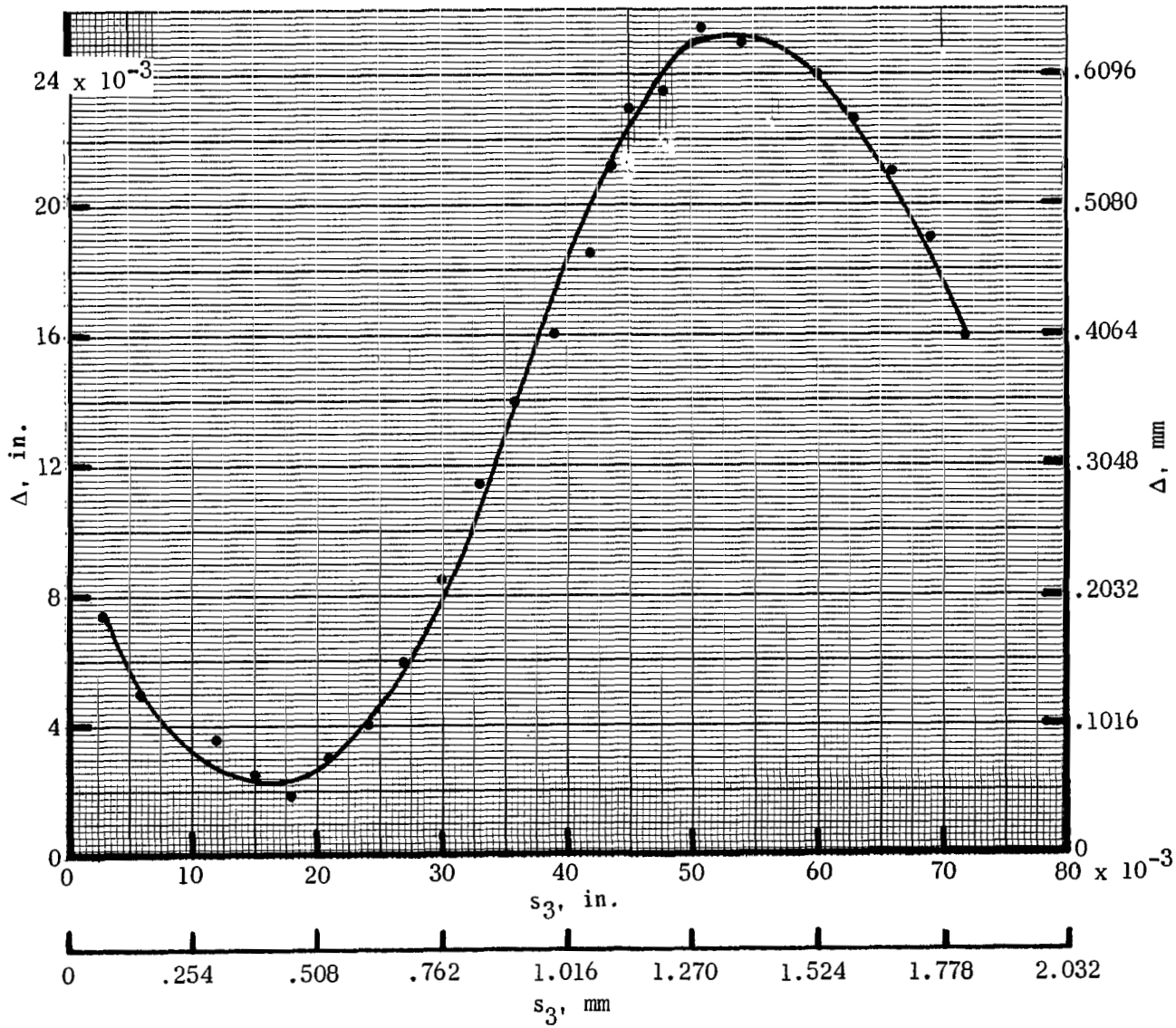

Figure 9.- Experimental curve of Δ necessary to restore resonance as a function of position of dielectric sheet for polystyrene. (s_1 = 2.010 in. (51.054 mm).)

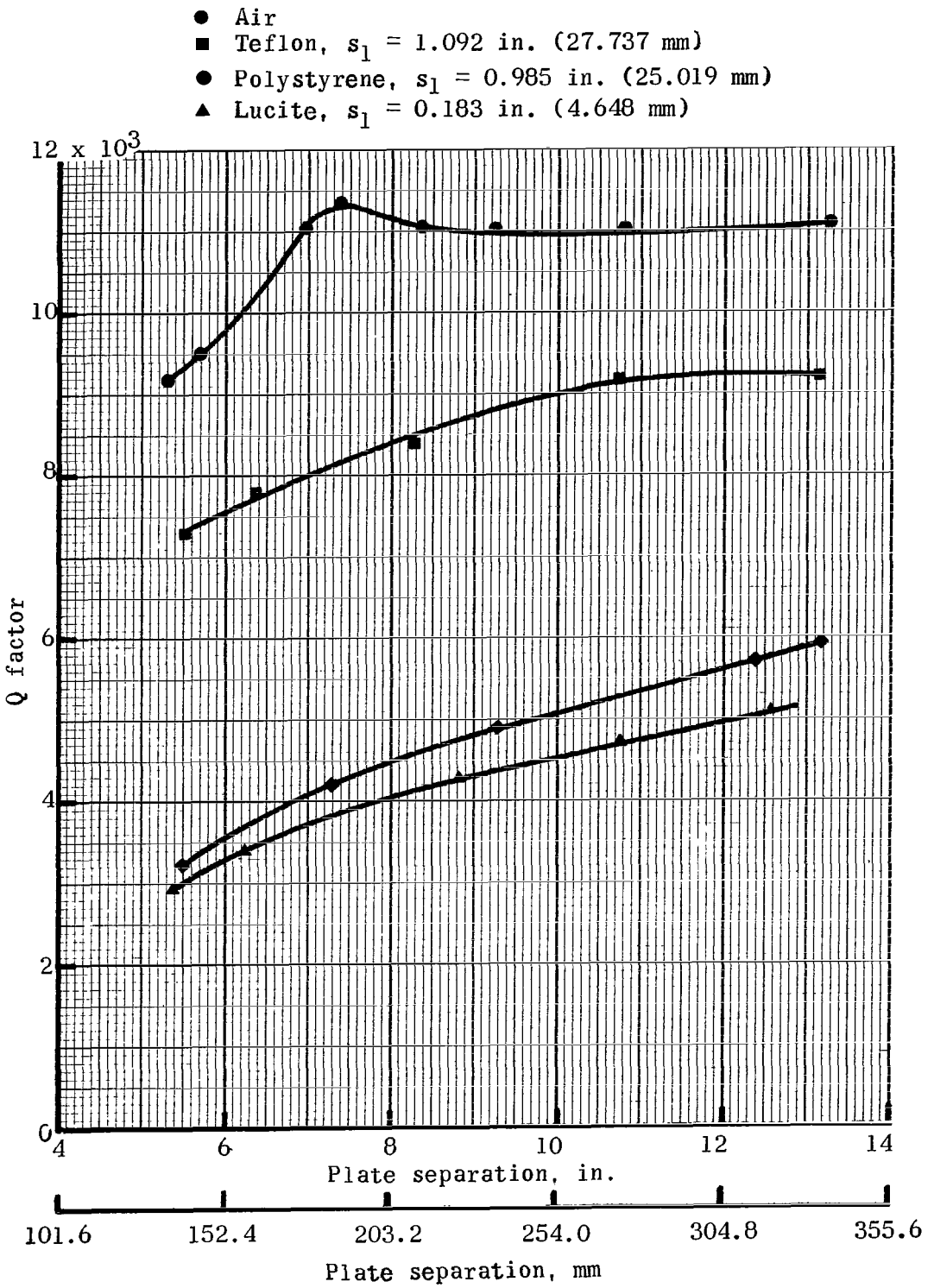

Figure 10.- Q factor as a function of plate separation for air and other dielectric sheets.

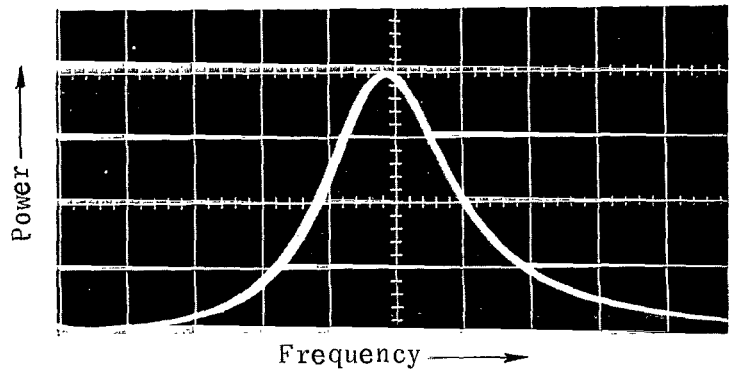

(a) Teflon. (1.092 in. (27.737 mm).) Q = 7042.

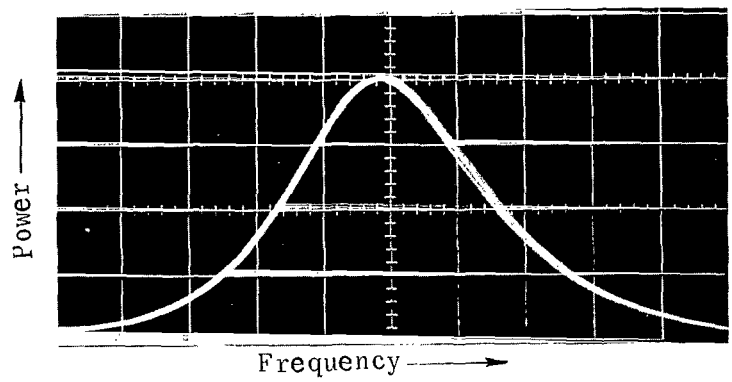

(b) Polystyrene. (1.012 in. (25.705 mm).) Q = 4049.

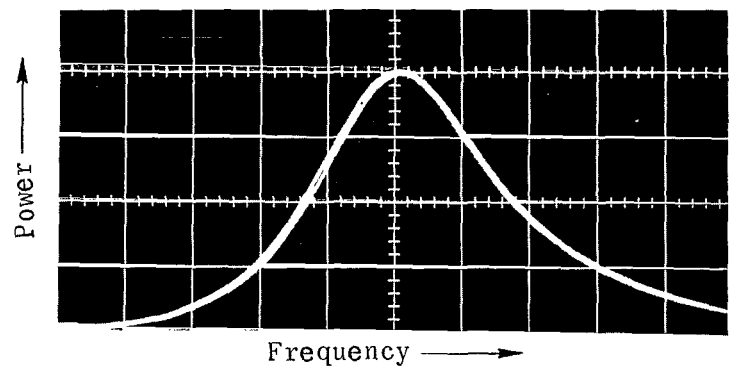

(c) Lucite. (0.123 in. (3.124 mm).) Q = 4407.

Figure 11.- Cavity response for different materials at 61 398 MHz.

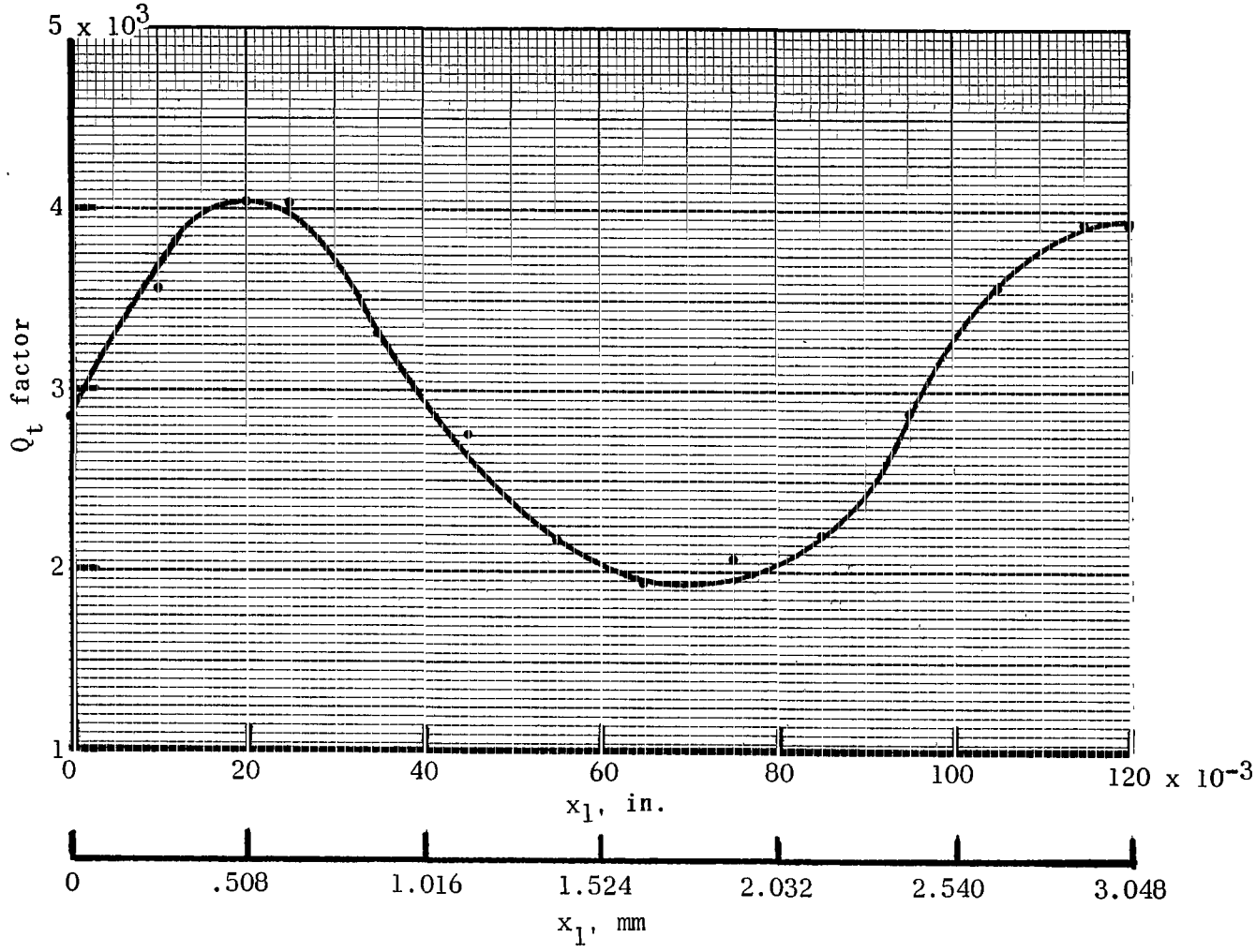

Figure 12.- Q_t factor as a function of relative position of dielectric sheet for lucite. (s_1 = 0.183 in. (4.648 mm).)

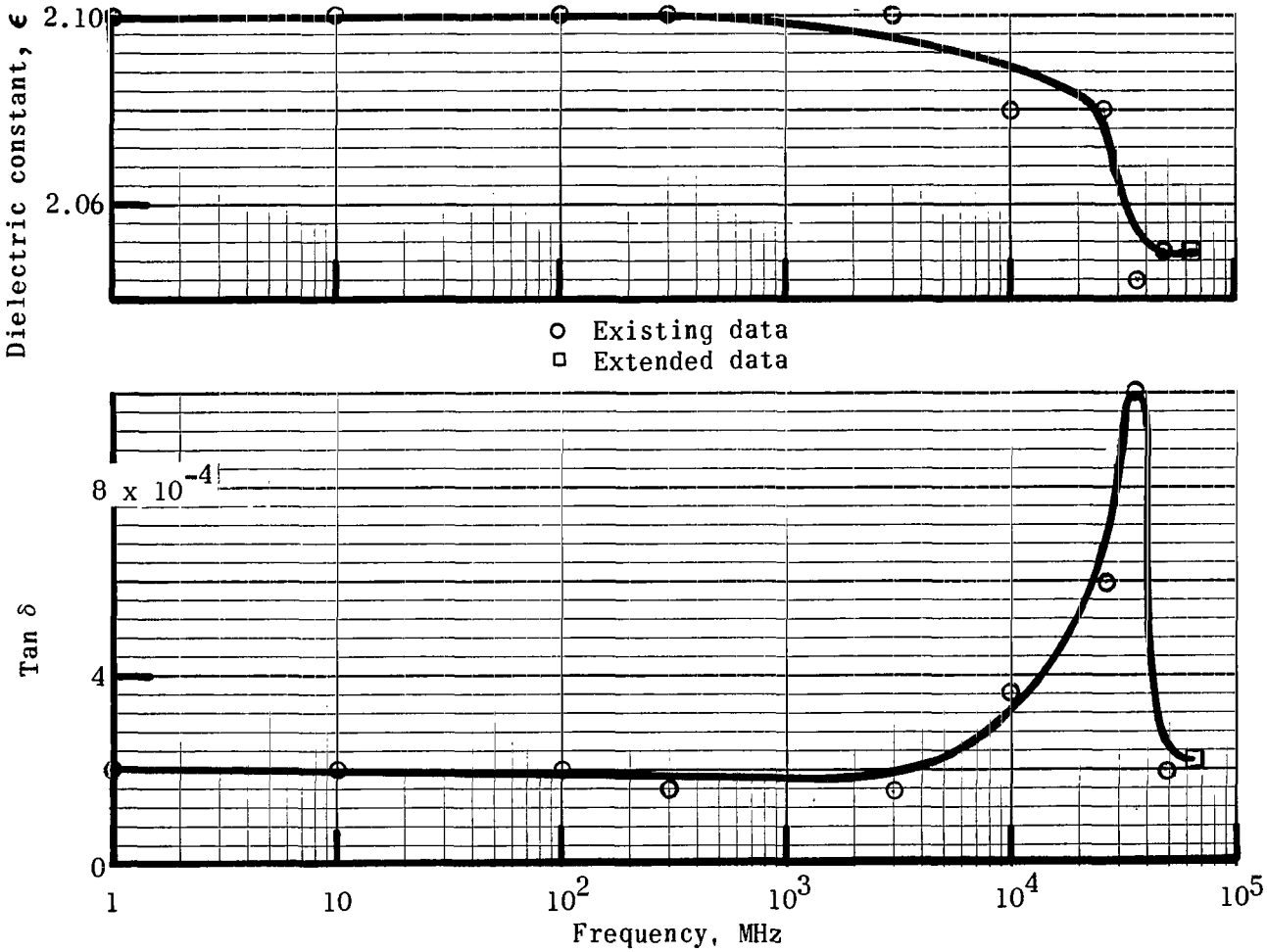

Figure 13.- Dielectric constant and loss tangent as functions of frequency for teflon.

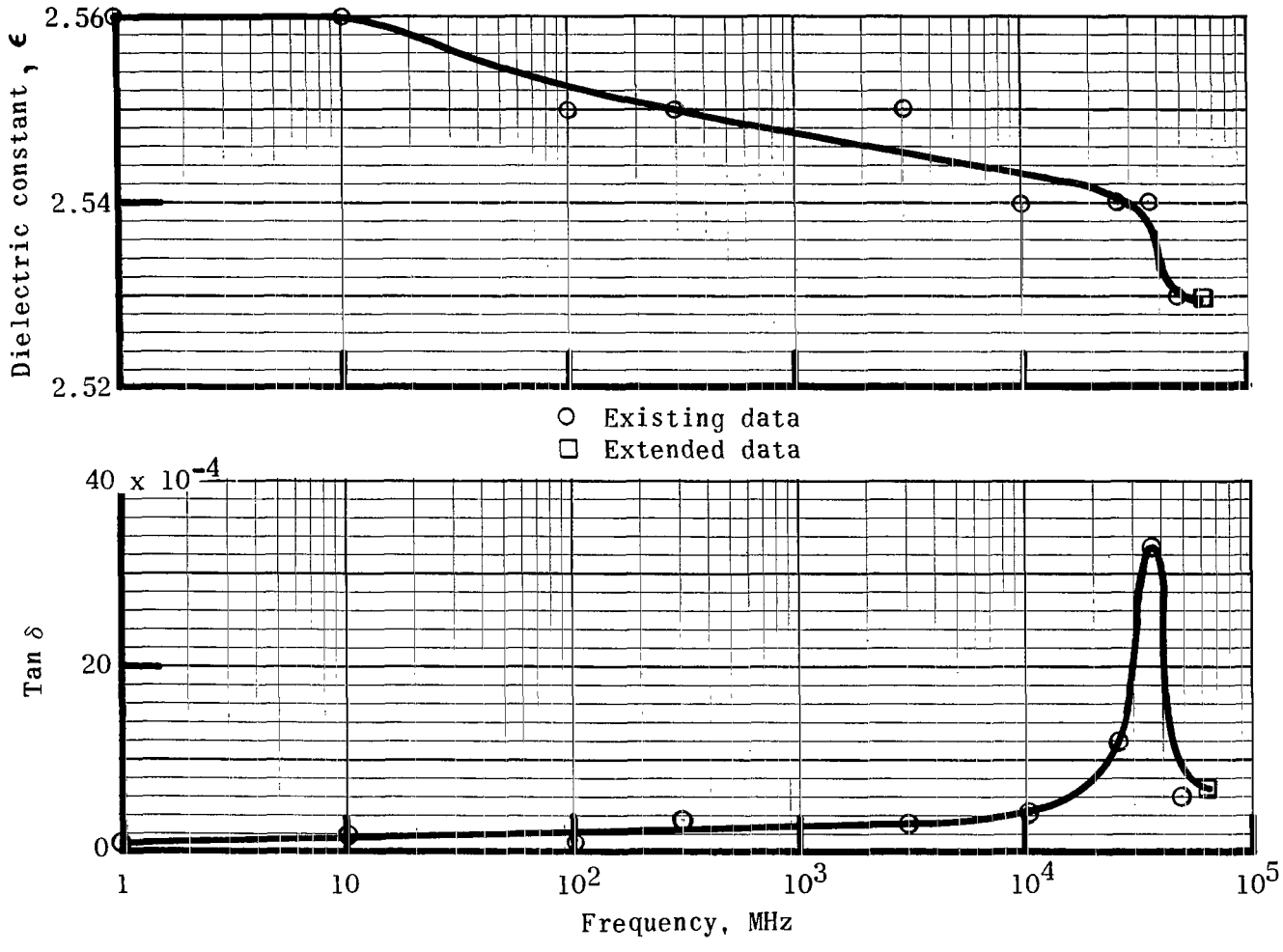

Figure 14.- Dielectric constant and loss tangent as functions of frequency for polystyrene.

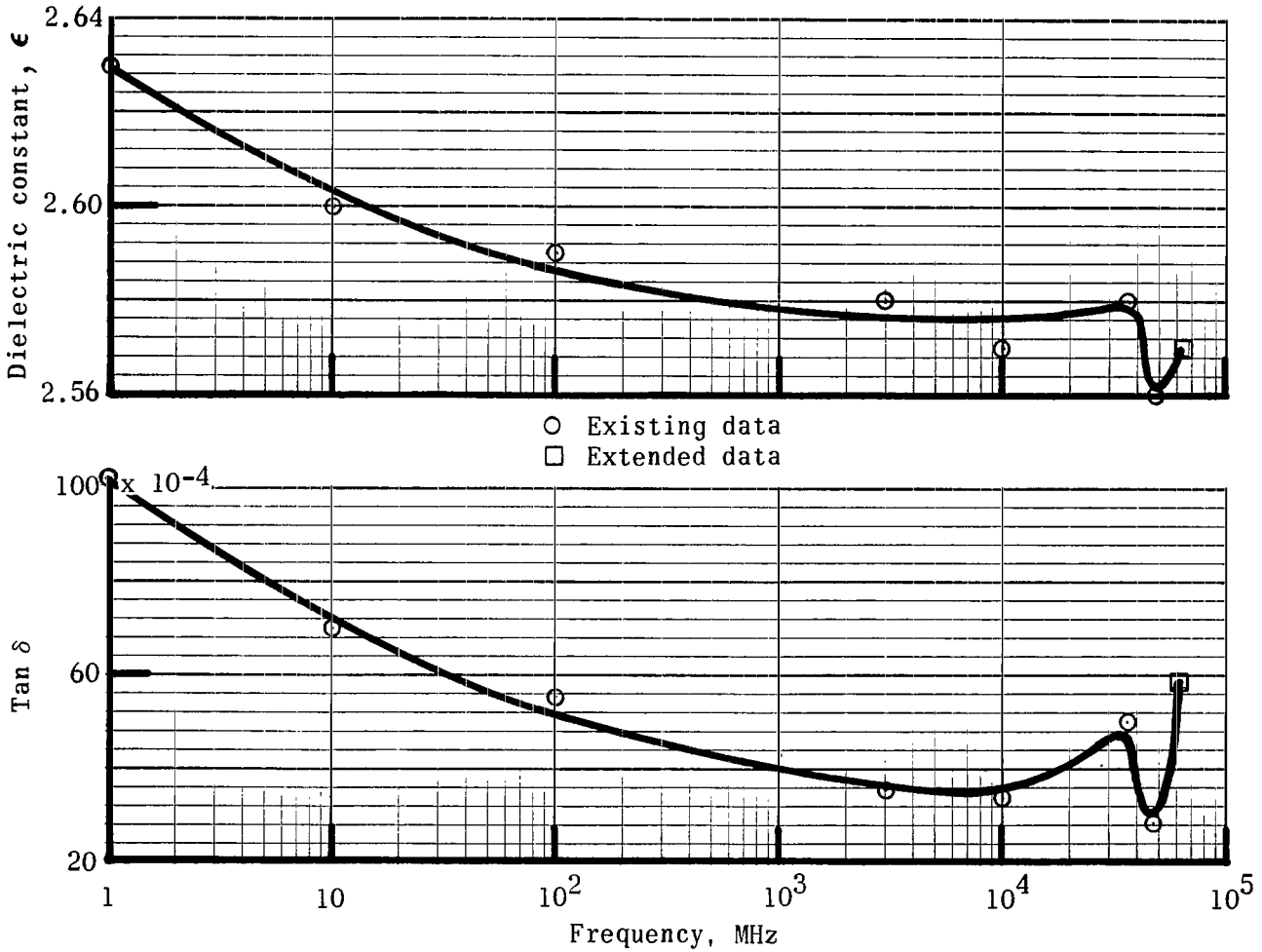

Figure 15.- Dielectric constant and loss tangent as functions of frequency for lucite.

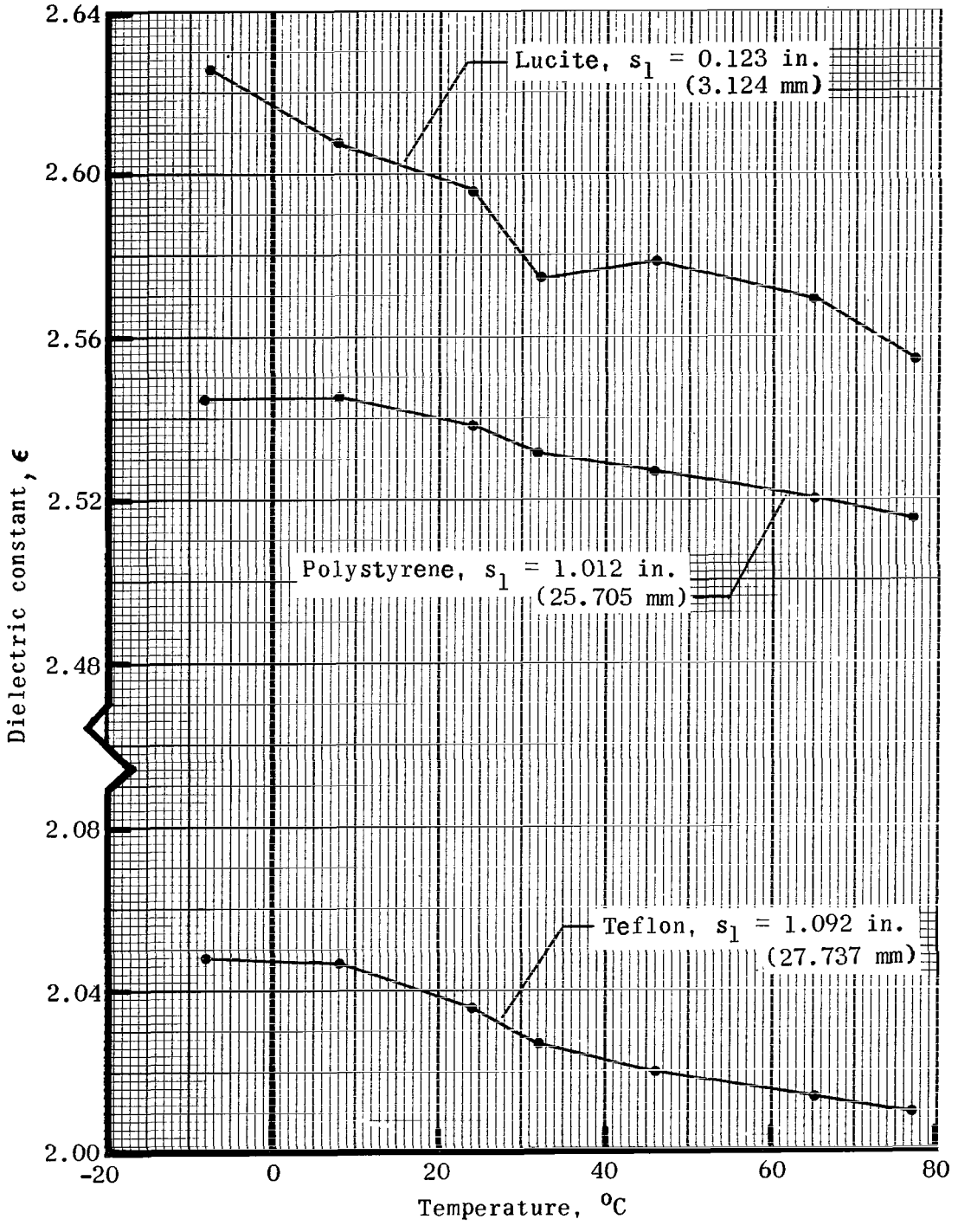

Figure 16.- Dielectric constant as a function of temperature at 61 242.103 MHz.

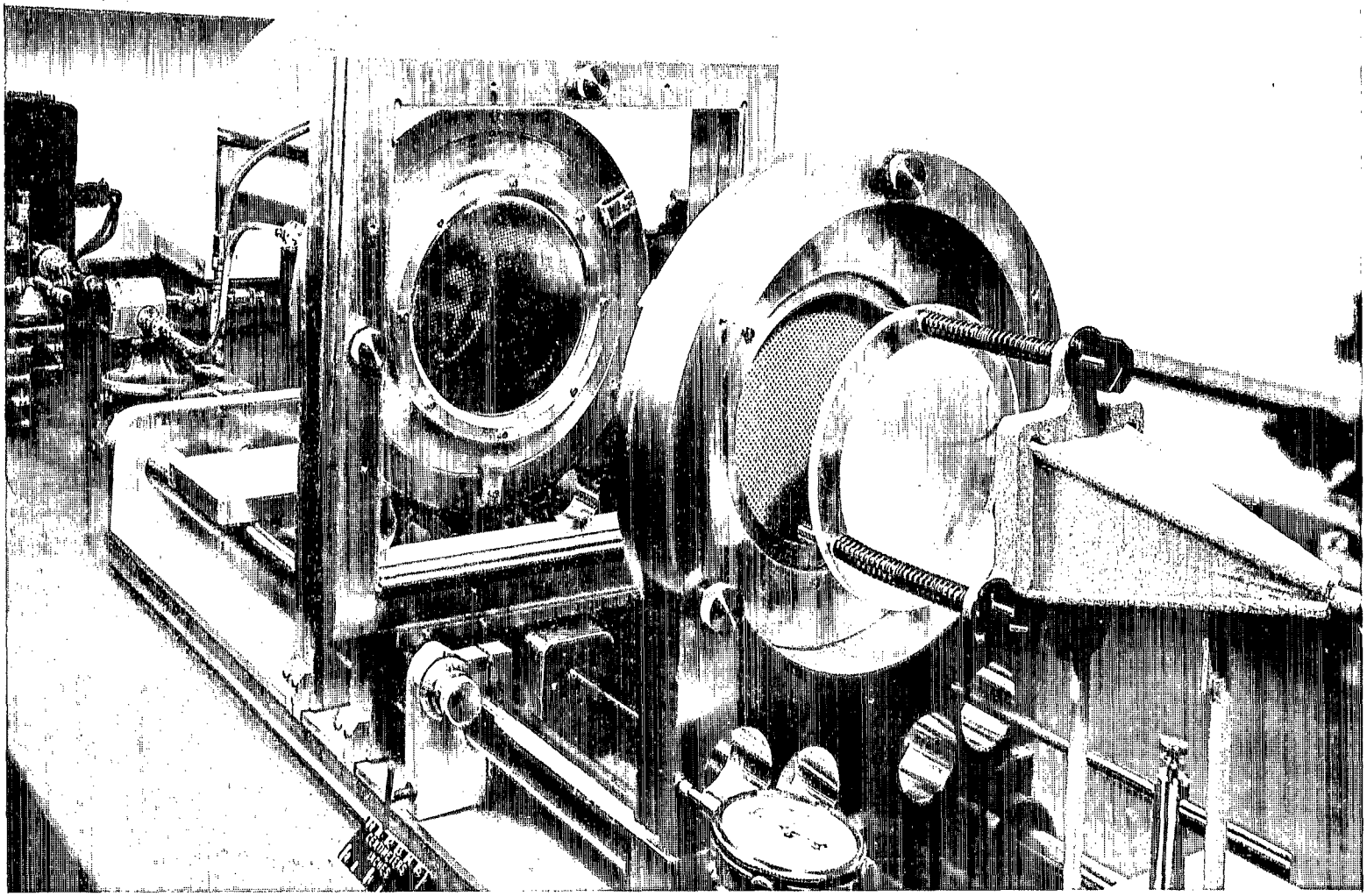

Figure 17.- Structure of a flat-plate Fabry-Perot resonant cavity. L-66-2981

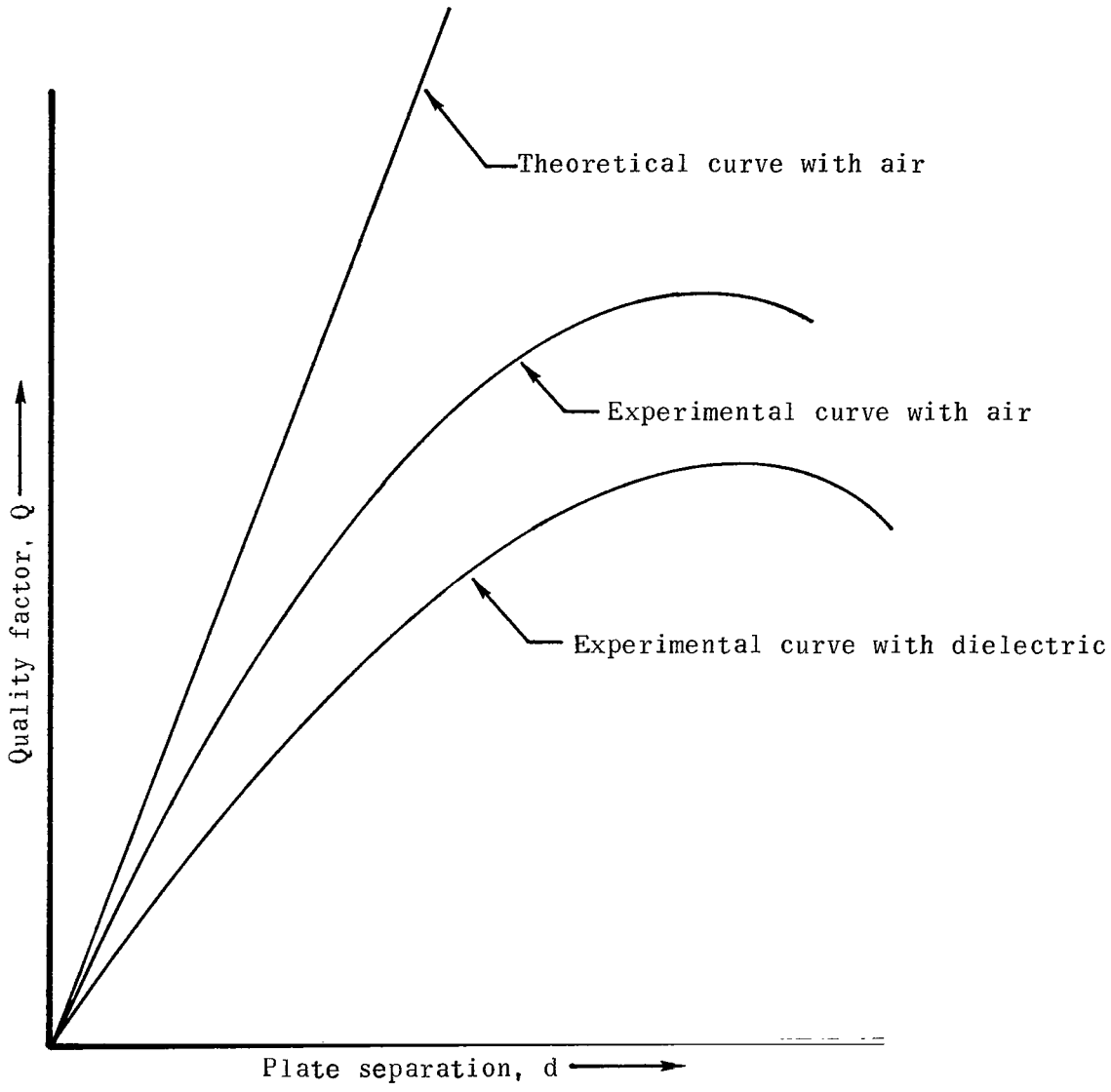

Figure 18.- Quality factor as a function of plate separation for flat-plate resonant cavity.

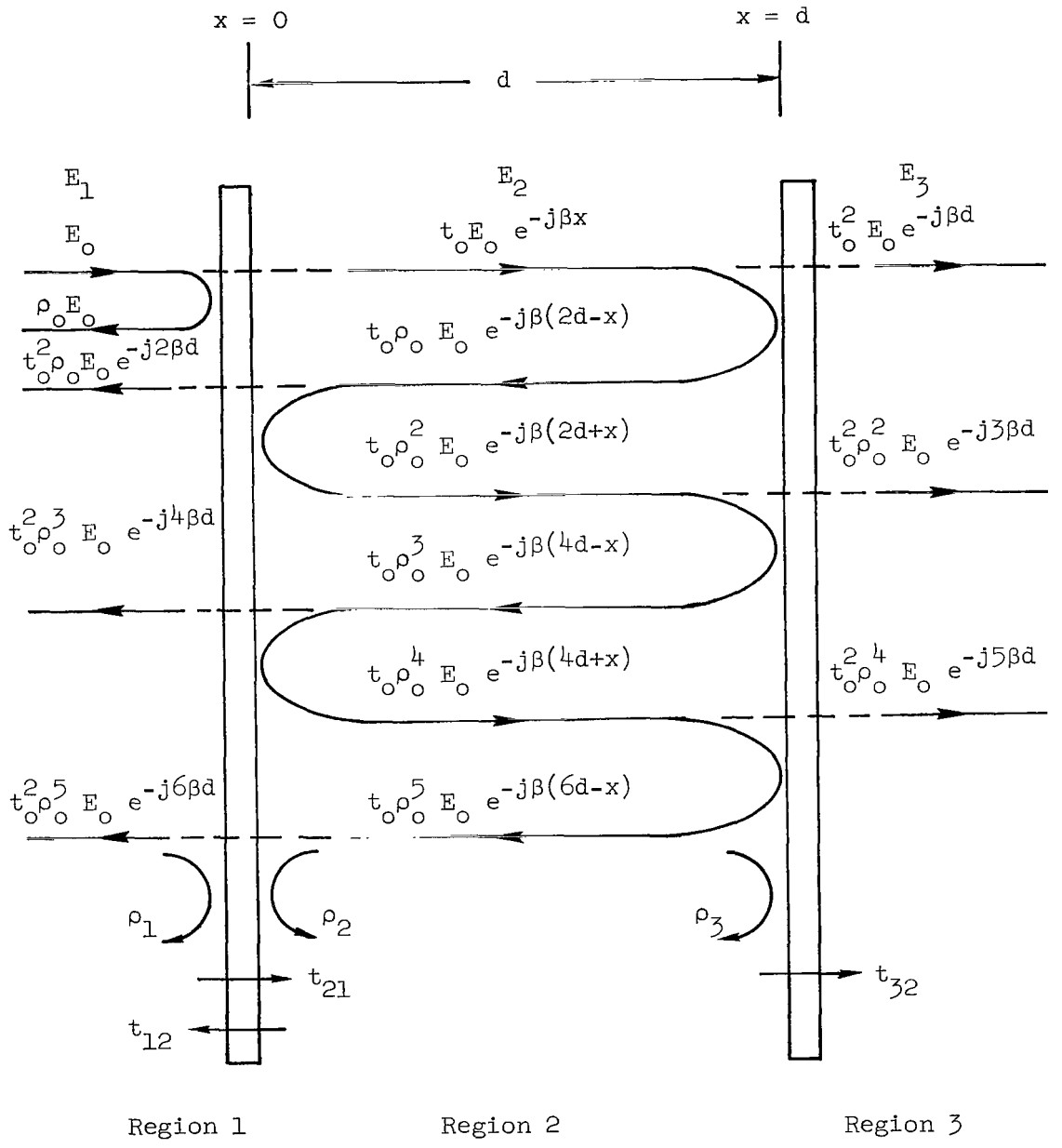

Figure 19.- Flat-plate resonant cavity.

NATIONAL AERONAUTICS AND SPACE ADMINISTRATION
WASHINGTON, D.C. 20546
OFFICIAL BUSINESS

FIRST CLASS MAIL

POSTAGE AND FEES PAID
NATIONAL AERONAUTICS AN
SPACE ADMINISTRATION

"The aeronautical and space activities of the United States shall be conducted so as to contribute . . . to the expansion of human knowledge of phenomena in the atmosphere and space. The Administration shall provide for the widest practicable and appropriate dissemination of information concerning its activities and the results thereof."

—NATIONAL AERONAUTICS AND SPACE ACT OF 1958

NASA SCIENTIFIC AND TECHNICAL PUBLICATIONS

TECHNICAL REPORTS: Scientific and technical information considered important, complete, and a lasting contribution to existing knowledge.

TECHNICAL NOTES: Information less broad in scope but nevertheless of importance as a contribution to existing knowledge.

TECHNICAL MEMORANDUMS: Information receiving limited distribution because of preliminary data, security classification, or other reasons.

CONTRACTOR REPORTS: Scientific and technical information generated under a NASA contract or grant and considered an important contribution to existing knowledge.

TECHNICAL TRANSLATIONS: Information published in a foreign language considered to merit NASA distribution in English.

SPECIAL PUBLICATIONS: Information derived from or of value to NASA activities. Publications include conference proceedings, monographs, data compilations, handbooks, sourcebooks, and special bibliographies.

TECHNOLOGY UTILIZATION PUBLICATIONS: Information on technology used by NASA that may be of particular interest in commercial and other non-aerospace applications. Publications include Tech Briefs, Technology Utilization Reports and Notes, and Technology Surveys.

Details on the availability of these publications may be obtained from:

SCIENTIFIC AND TECHNICAL INFORMATION DIVISION

NATIONAL AERONAUTICS AND SPACE ADMINISTRATION

Washington, D.C. 20546